PHOTOMETRIC INVESTIGATION OF A VERY SHORT PERIOD W UMa-TYPE BINARY: DOES CE LEONIS HAVE A LARGE SUPERLUMINOUS AREA?

RONALD G. SAMEC[1,2]
Department of Physics and Astronomy, Millikin University, Decatur, Illinois 62522
Electronic mail: rsamec@mail.millikin.edu

WEN SU
Department of Physics and Astronomy, University of Kentucky, Lexington, Kentucky 40506
Electronic mail: wsu00@ukcc.uky.edu

DIRK TERRELL
Department of Astronomy, University of Florida, Gainesville, Florida 32609
Electronic mail: terrell@astro.ufl.edu

DOUGLAS P. HUBE[2]
Department of Physics, University of Alberta, Edmonton, Alberta, T6G 2J1, Canada
Electronic mail: userpuls@mts.ucs.ualberta.ca

Received 1992 June 12; revised 1993 March 3

ABSTRACT

A complete photometric analysis of *BVRI* Johnson–Cousins photometry of the high northern latitude galactic variable, CE Leo is presented. These observations were taken at Kitt Peak National Observatory on 1989 May 31–1989 June 7. Three new precise epochs of minimum light were determined and a linear and a quadratic ephemeris were computed from these and previous data covering 28 years (>33 000 revolutions) of observation. The light curves reveal that the system undergoes a brief 20 min totality in the primary eclipse, indicating that CE Leo is a W UMa W-type binary. A systemic velocity of ~ -40 km/s was determined. Standard magnitudes were found and a simultaneous solution of the *B*, *V*, *R*, *I* light curves was computed using the new Wilson–Devinney synthetic light curve code which has the capability of automatically adjusting star spots. The solution indicates that the system consists of two early K-type dwarfs in marginal contact with a fill-out factor less than 3%. Evidence for the presence of a large (45° radius) superluminous area on the cooler component is given.

1. INTRODUCTION

The very short period binary, CE Leonis [S 7763, $\alpha(1950)=11^h41^m\ 50^2$, $\delta(1950)=23°36'10''$], was discovered by Hoffmeister (1963) in a search for variables near the north galactic pole [galactic latitude, $\beta=+74°.31$]. This variable was originally classified RRc-type but later identified as W UMa-type, i.e., EW-type, by Wenzel & Zeigler (1966). They list the first published ephemeris:

$$\text{JD (hel.) Min I}=2437651^d.650+0.3034286\cdot E. \quad (1)$$

The 22 timings of minimum used to calculate this ephemeris are given in the report of Meinunger & Wenzel (1968). They give a visual light curve, noting both the magnitude range of the variable, $11^m.8$ to $12^m.6$, and the depth of the secondary eclipse, $0^m.7$. Eleven visual timings of minimum light are given in the BBSAG bulletins No. 9, 14, 15, 21, 37, and 92. Two epochs of minimum light have been published by Hoffmann (1983) from his *B,V* photoelectric observations which are available on microfilm (Hoffmann 1984). One other epoch is provided by Samec & Bookmyer (1987a) along with *BVRI* partial light curves from their photoelectric observations covering the secondary eclipse, $0^p.5$ or Min II, and the maximum at $0^p.25$, or Max I. (Similarly, in this paper, Min I refers to the deepest part of the eclipse curve, $0^p.0$ and Max II refers to the maximum following the secondary eclipse, $0^p.75$.) These precise curves confirm that CE Leo is an EW-type variable. The depth of the secondary eclipse (Max I–Min II) in *V* is $0^m.66$. No further references are available on this neglected twelfth magnitude system. The observations presented here represent the first complete precise light curves and the first spectroscopic information available on the system.

2. OBSERVATIONS

The observations of CE Leo were made on 1989 May 30–1989 June 3, inclusive, and 1989 June 5&6, at Kitt Peak National Observatory (KPNO), Tucson, Arizona. The 0.9 m No. 2 *f*/7.5 reflector (now retired) was used in conjunction with the Automated Filter Photometer (AFP2), hous-

[1]Visiting Astronomer, Kitt Peak National Observatory, National Optical Astronomical Observatories, which are operated by the Association of Universities for Research in Astronomy, Inc. under contract with the National Science Foundation.
[2]Guest investigator at the Dominion Astrophysical Observatory.

 0004-6256/93/106(1)/318/19/$0.90

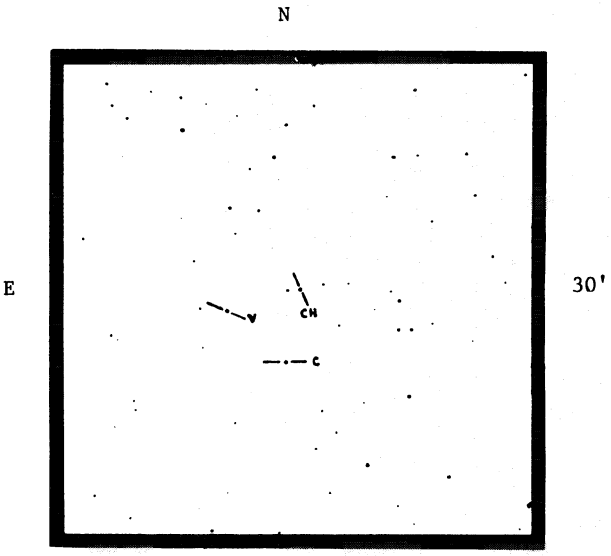

FIG. 1. Finding chart of CE Leonis (v), the comparison star (c), and the check star (ch).

ing a dry-ice-cooled RCA 31034A-02 Ga–AS PMT (cold box #51). The photometry was done on the Johnson–Cousins system (Landolt 1983; Bessell 1976, 1979) with the Bessell–KPNO *B,V,R,I* filter set. Data acquisition was semiautomated, with user-written program sequences utilizing the KPNO Photometry Control Program. The procedures followed are similar to those detailed previously (Samec & Bookmyer 1987b). Standard differential photometry was done with a repeated sky-comp-variable sequence. The check star was monitored at 2 or 3 h intervals. The comparison star and sky were observed at 5–7 min intervals bracketing 2–3 variable star *IRVB* measurements. A single variable star observation consisted of a 4 s integration in both *I* and *R*, 6 s in *V*, and 12 s in *B*. At no time did the variable minus sky reading in any filter drop below a minimum count of 10 000, even during primary eclipse, so that photon noise should not keep the photometric precision from being as good as 1%. A focal plane diaphragm with an aperture of 25 arcsec in diameter was used for all observations.

Two nearby stars, within about 15 arcmin, and identified in an earlier report (Samec & Bookmyer 1987a), were used as check and comparison stars. The eleventh magnitude star whose position is $\alpha(1950) \sim 11^h41^m33^s$, $\delta(1950) \sim 23°32'36''$ was chosen as the comparison star since it provided an excellent color match for the variable with $\Delta(B-V) \sim -0.1$ and $\Delta(R-I) \sim 0^m0$. The somewhat bluer [$\Delta(B-V) \sim 0^m34$, $\Delta(R-I) \sim 0^m15$], twelfth magnitude star, whose position is $\alpha(1950) \sim 11^h41^m27^s$, $\delta(1950) \sim 23°37'24''$, was used as the check star. Measurements of the check star indicated that the light of the comparison star stayed constant at least within scatter bands of $\sim \pm 0^m01$ in *V* throughout the observing interval. A finding chart is given as Fig. 1 designating the variable, comparison, and check star as v, c, and ch, respectively. Differential extinction corrections were found to be negligible ($< 0^m01$) and were not applied to the observations. The individual observations, 529 with both the *B* and *V* filters, 570 with the *R* filter, and 563 with the *I* filter are listed in Table 1 as Heliocentric Julian Date (HJD) versus magnitude difference, is Delta Mag. The latter is given as variable minus comparison star, v−c. A number of *B,V* observations made on June 5 at very large airmasses and found to be highly variable in the counts, were removed from the analysis. This accounts for the fewer observations in *B,V* than in *R,I*.

As mentioned in our recent spectroscopic-radial velocity study of BX Peg (Samec & Hube 1991), CE Leo was also observed, spectroscopically as well, using the same procedures, telescope (the 1.88 m reflector at Dominion Astrophysical Observatory), CCD instrumentation, and reduction techniques as with BX Peg. We failed to detect the presence of double spectral components in any of the exposures or cross-correlation functions. Even though the two stars are comparatively bright, they are intrinsically faint. A larger telescope and better S/N will be needed. We did, however, estimate the systemic velocity to be −40 km/s. This value will be useful in the determination of the space motion of the variable.

3. STANDARD MAGNITUDES

Five to twelve standard star measurements of Landolt (1983) $UBVR_cI_c$ photometric standards were taken every evening. The stars observed included the HD stars 10258, 103462, 103302, 103526, 10566, 105205, 105405, 105448, 105663, 1061024, 107347, 107595, 108475, 108551, 108702, 1081332, 1112009, 1112512, 1112522, 111717, 111775, 1112522, 121960, 148817, 149382, and BD+5 2529. Primary extinction coefficients, which were used in the calculation of nightly transformations (Hardie 1962), were determined from nightly comparison star measurements. The transformation coefficients, when applied to the standard stars, reproduced their standard magnitudes quite well, with residuals of ±1 to ±10 mmag. The coefficients were then used in the calculation of standard values of the variable, check, and comparison star. This information is given in Table 2. The magnitudes of the comparison and check star are mean values of determinations from the most stable nights, 102 for the comparison and 10 for the check star. Each variable star standard magnitude is the mean calculated from 5–10 determinations occurring within $\sim \pm 0^m02$ of the phase in question. In Table 2 and throughout this paper, values are accompanied by their probable errors shown in parentheses. Both the high galactic latitude and the (*B*−*V*), (*R*−*I*), and (*V*−*I*) color indices would suggest that there is negligible interstellar reddening of the variable, comparison, and check star. At phase 0^m0, the primary (occulting) component has color indices (Popper 1980; Bessell 1979) which indicate spectral type K2(V). The ratio of fluxes from our light curve solution (Model II) given later in this paper was used to determine that the secondary component is type K1 (V). The comparison star is of spectral type K3 (V) and the check star is an early G (V)-type [in the G0 (V) to G4

TABLE 1. Observations of CE Leonis.

B Observations

JD HEL. 2447670+	DELTA B MAG	JD HEL. 2447670+	DELTA B MAG	JD HEL. 2447670+	DELTA B MAG	JD HEL. 2447670+	DELTA B MAG	JD HEL. 2447670+	DELTA B MAG
7.70726	0.93641	8.77945	0.73015	9.69916	0.54034	9.74190	0.24570	10.67884	0.34391
7.70765	0.94172	8.77983	0.72199	9.70135	0.50126	9.74246	0.27541	10.67943	0.34387
7.70817	0.90556	8.78185	0.64222	9.70174	0.50609	9.74284	0.27075	10.67980	0.35256
7.70854	0.91033	8.78224	0.63479	9.70230	0.48992	9.74497	0.26737	10.68177	0.36062
7.71479	0.79235	8.78291	0.61659	9.70267	0.50534	9.74536	0.27953	10.68215	0.36695
7.71517	0.76910	8.78329	0.64237	9.70464	0.43798	9.74603	0.26854	10.68273	0.34954
7.71574	0.77116	8.78633	0.59288	9.70502	0.44149	9.74641	0.27541	10.68311	0.36138
7.71612	0.74221	8.78671	0.60353	9.70560	0.45803	9.74848	0.28593	10.68503	0.36847
7.71809	0.69422	8.78880	0.56264	9.70597	0.43208	9.74887	0.27526	10.68495	0.44679
7.71848	0.69467	8.78919	0.56161	9.70801	0.41947	9.74946	0.26096	10.68543	0.36831
7.71920	0.69100	8.78991	0.55202	9.70840	0.41633	9.74984	0.24937	10.68602	0.39110
7.71957	0.68041	8.79029	0.53525	9.70895	0.42526	9.75188	0.27125	10.68639	0.38028
7.72185	0.65730	9.66684	1.16158	9.70933	0.41307	9.75226	0.26487	10.68841	0.41175
7.72223	0.61695	9.66809	1.16939	9.71124	0.38698	9.75286	0.28861	10.68879	0.39867
7.72281	0.63968	9.66847	1.15228	9.71162	0.40592	9.75324	0.29257	10.68935	0.40961
7.72319	0.62471	9.67043	1.16211	9.71220	0.39089	9.75519	0.29661	10.68973	0.39796
7.72547	0.58009	9.67082	1.13873	9.71257	0.40283	9.75558	0.29795	10.69165	0.41738
7.72586	0.57078	9.67144	1.14341	9.71453	0.38764	9.75624	0.28415	10.69203	0.42397
7.72642	0.58252	9.67182	1.14123	9.71492	0.40146	9.75661	0.27862	10.69264	0.44532
7.72680	0.56352	9.67394	1.15835	9.71550	0.37843	9.75867	0.31344	10.69302	0.41885
7.72876	0.55727	9.67432	1.16202	9.71588	0.37800	9.75906	0.30264	10.69494	0.44412
7.72915	0.55422	9.67489	1.17030	9.71788	0.38717	9.75963	0.32399	10.69533	0.44992
7.72978	0.54878	9.67527	1.15207	9.71827	0.35959	9.76001	0.32884	10.69614	0.43060
7.73016	0.52559	9.67747	1.11257	9.71889	0.37291	9.76198	0.33814	10.69652	0.47312
7.73254	0.53780	9.67786	1.11019	9.71926	0.33837	9.76237	0.33280	10.69861	0.44584
7.73293	0.51906	9.67852	1.07160	9.72121	0.34718	9.76293	0.31567	10.69899	0.47483
7.73350	0.50949	9.67889	1.03928	9.72160	0.31376	9.76331	0.32743	10.69992	0.47883
7.73388	0.49693	9.68089	0.97764	9.72235	0.31756	9.76557	0.34301	10.70029	0.49127
8.76090	1.19576	9.68128	0.98575	9.72273	0.29160	9.76596	0.33656	10.70237	0.51637
8.76129	1.19358	9.68192	0.94573	9.72493	0.32146	9.76654	0.33737	10.70276	0.51678
8.76263	1.19064	9.68229	0.95128	9.72532	0.33940	9.76691	0.33839	10.70335	0.54549
8.76301	1.18881	9.68434	0.90484	9.72587	0.32046	9.76884	0.33371	10.70372	0.53082
8.76490	1.13069	9.68473	0.89030	9.72625	0.30803	9.76922	0.34706	10.70578	0.57290
8.76530	1.16337	9.68532	0.85932	9.72822	0.32060	9.76979	0.34932	10.70616	0.59000
8.76586	1.15630	9.68569	0.86469	9.72860	0.32732	9.77016	0.37579	10.70677	0.58145
8.76624	1.11030	9.68772	0.80831	9.72918	0.30969	9.77224	0.32917	10.70715	0.60285
8.76829	1.09585	9.68811	0.79267	9.72955	0.32803	9.77263	0.32966	10.70907	0.64273
8.76868	1.06550	9.68872	0.75929	9.73150	0.35235	9.77326	0.36715	10.70946	0.62542
8.76931	1.03846	9.68910	0.76490	9.73189	0.33124	9.77364	0.33904	10.71006	0.68415
8.76968	1.04767	9.69114	0.70157	9.73245	0.31740	9.77571	0.38661	10.71043	0.65309
8.77168	0.97923	9.69153	0.70595	9.73283	0.30436	9.77610	0.40832	10.71240	0.71445
8.77207	0.98210	9.69208	0.68206	9.73480	0.31335	9.77671	0.42058	10.71279	0.70618
8.77264	0.93244	9.69245	0.67725	9.73519	0.28645	9.77708	0.41518	10.71351	0.71873
8.77302	0.96729	9.69453	0.63901	9.73575	0.29803	9.77919	0.43505	10.71389	0.72639
8.77507	0.86957	9.69492	0.63676	9.73612	0.29846	9.77958	0.43830	10.71590	0.79074
8.77546	0.84185	9.69547	0.59249	9.73808	0.27627	10.67521	0.31843	10.71629	0.76988
8.77604	0.82922	9.69585	0.58644	9.73847	0.27045	10.67559	0.31943	10.71684	0.79733
8.77642	0.86547	9.69784	0.54867	9.73902	0.28424	10.67620	0.33544	10.71722	0.80058
8.77853	0.75677	9.69823	0.55278	9.73940	0.26927	10.67657	0.32012	10.71915	0.84862
8.77892	0.74896	9.69878	0.53366	9.74151	0.26377	10.67845	0.34120	10.71954	0.82065

TABLE 1. (continued)

JD HEL. 2447670+	DELTA B MAG	JD HEL. 2447670+	DELTA B MAG	JD HEL. 2447670+	DELTA B MAG	JD HEL. 2447670+	DELTA B MAG	JD HEL. 2447670+	DELTA B MAG
10.72013	0.87761	10.76594	0.54252	11.69536	0.38663	11.73446	0.34272	11.77907	0.96298
10.72051	0.86457	10.76632	0.55136	11.69547	0.41950	11.73658	0.39212	11.77917	0.96155
10.72241	0.93864	10.76843	0.49228	11.69628	0.38195	11.73668	0.41792	11.77997	0.98337
10.72280	0.91863	10.76882	0.51001	11.69636	0.40428	11.73761	0.40490	11.78005	0.95840
10.72341	0.90321	10.76941	0.49739	11.69718	0.35822	11.73842	0.39008	11.78090	1.01545
10.72379	0.94233	10.76979	0.51443	11.69727	0.39551	11.73851	0.38348	11.78098	0.99609
10.72571	0.97866	10.77685	0.44046	11.70003	0.36819	11.74058	0.41819	11.78315	1.06017
10.72611	1.00858	10.77723	0.42832	11.70013	0.35806	11.74068	0.38028	11.78325	1.08757
10.72667	0.99009	10.77779	0.41631	11.70089	0.36761	11.74146	0.38614	11.78415	1.09730
10.72704	0.97072	10.77816	0.42833	11.70098	0.35130	11.74155	0.41260	11.78720	1.13030
10.72889	1.03468	10.78010	0.39673	11.70177	0.36851	11.74284	0.41678	11.78730	1.16471
10.72928	1.03036	10.78050	0.41837	11.70186	0.34274	11.70804	0.37724	11.78897	1.19665
10.72988	1.04151	10.78108	0.40711	11.70395	0.37675	11.74294	0.47239	13.72598	0.42605
10.73026	1.02295	10.78146	0.42672	11.70405	0.36710	11.75016	0.47711	13.72615	0.43118
10.73219	1.07876	10.78359	0.38787	11.70486	0.35870	11.75026	0.45139	13.72692	0.42719
10.73258	1.03200	10.78398	0.40647	11.70496	0.35780	11.75121	0.45292	13.72708	0.42583
10.73317	1.07364	10.78463	0.41022	11.70578	0.34992	11.75130	0.46229	13.72786	0.44440
10.73355	1.04187	10.78501	0.39013	11.70587	0.34086	11.75210	0.47180	13.72803	0.43840
10.73541	1.03506	11.67103	0.54833	11.70804	0.37724	11.75220	0.45911	13.73013	0.45099
10.73580	1.02909	11.67113	0.57730	11.70814	0.34839	11.75442	0.50814	13.73030	0.46589
10.73637	1.06880	11.67190	0.57626	11.70891	0.35078	11.75452	0.48593	13.73113	0.46249
10.73674	1.05983	11.67199	0.55958	11.70900	0.32789	11.75530	0.50042	13.73129	0.46461
10.73869	0.99629	11.67285	0.54282	11.70981	0.33236	11.75539	0.48515	13.73212	0.46766
10.73907	0.98142	11.67294	0.55448	11.70990	0.33391	11.75624	0.51066	13.73228	0.48730
10.73962	1.02154	11.67503	0.53606	11.71199	0.32719	11.75633	0.51519	13.73443	0.49960
10.73999	0.96227	11.67514	0.53084	11.71209	0.30498	11.75850	0.49121	13.73460	0.50652
10.74185	0.90103	11.67591	0.51570	11.71286	0.30424	11.75860	0.51214	13.73541	0.50593
10.74224	0.91179	11.67600	0.53211	11.71295	0.30229	11.75939	0.52328	13.73556	0.51007
10.74277	0.88279	11.67689	0.50993	11.71383	0.32182	11.75948	0.54056	13.73639	0.51016
10.74315	0.87696	11.67697	0.52548	11.71392	0.32190	11.76039	0.51059	13.73655	0.52370
10.74506	0.81500	11.67911	0.50957	11.71602	0.37270	11.76049	0.54079	13.73873	0.54002
10.74545	0.83109	11.67921	0.48974	11.71613	0.35447	11.76269	0.59026	13.73890	0.53396
10.74605	0.82744	11.68001	0.46881	11.71698	0.35727	11.76279	0.58691	13.73971	0.56356
10.74642	0.81195	11.68010	0.48840	11.72013	0.32978	11.76363	0.56608	13.73987	0.56608
10.74838	0.73061	11.68096	0.45734	11.72024	0.34729	11.76372	0.58358	13.74066	0.57572
10.74877	0.73145	11.68105	0.48100	11.72107	0.30561	11.76452	0.60576	13.74082	0.59140
10.74938	0.74496	11.68332	0.45202	11.72116	0.32793	11.76461	0.58488	13.74177	0.58294
10.74976	0.76134	11.68341	0.44901	11.72197	0.31374	11.76679	0.66203	13.74193	0.58766
10.75170	0.74751	11.68420	0.46940	11.72206	0.32242	11.76689	0.62783	13.74271	0.61317
10.75208	0.71609	11.68429	0.47204	11.72437	0.37169	11.76769	0.66910	13.74286	0.60630
10.75265	0.68481	11.68510	0.42350	11.72514	0.38165	11.76778	0.65591	13.74363	0.62629
10.75302	0.69569	11.68519	0.42819	11.72523	0.33455	11.76859	0.66761	13.74378	0.63679
10.75495	0.70948	11.68738	0.42302	11.72607	0.37481	11.76868	0.70811	13.74591	0.65603
10.75533	0.65105	11.68748	0.44276	11.72616	0.34743	11.77092	0.70661	13.74609	0.65866
10.75595	0.65358	11.68834	0.42092	11.72847	0.41682	11.77102	0.71927	13.74686	0.68935
10.75633	0.71655	11.68843	0.40618	11.72928	0.33998	11.77182	0.74816	13.74701	0.68323
10.75834	0.59998	11.68921	0.41395	11.72937	0.36860	11.77191	0.74713	13.74779	0.69778
10.75873	0.58232	11.68930	0.43307	11.73017	0.33188	11.77272	0.76544	13.74795	0.70551
10.75935	0.59077	11.69144	0.44258	11.73026	0.36369	11.77281	0.78397	13.74880	0.70364
10.75973	0.61511	11.69154	0.44610	11.73257	0.37598	11.77497	0.83547	13.74896	0.70936
10.76265	0.54127	11.69234	0.47412	11.73267	0.40688	11.77507	0.81591	13.74972	0.72747
10.76303	0.51207	11.69243	0.46840	11.73347	0.31883	11.77597	0.92518	13.74988	0.73860
10.76502	0.49215	11.69320	0.44073	11.73357	0.34442	11.77682	0.88142	13.75067	0.76775
10.76541	0.50199	11.69329	0.43684	11.73438	0.32580	11.77691	0.88898	13.75082	0.78930

TABLE 1. (continued)

JD HEL. 2447670+	DELTA B MAG	JD HEL. 2447670+	DELTA B MAG	JD HEL. 2447670+	DELTA B MAG	JD HEL. 2447670+	DELTA B MAG	JD HEL. 2447670+	DELTA B MAG
13.75296	0.80191	13.75696	0.91366	13.74591	0.65603	13.74988	0.73860	13.75588	0.89540
13.75312	0.82258	13.75777	0.93994	13.74609	0.65866	13.75067	0.76775	13.75604	0.87846
13.75391	0.81772	13.75793	0.94417	13.74686	0.68935	13.75082	0.78930	13.75680	0.91519
13.75406	0.82437	13.74177	0.58294	13.74701	0.68323	13.75296	0.80191	13.75696	0.91366
13.75486	0.86899	13.74193	0.58766	13.74779	0.69778	13.75312	0.82258	13.75777	0.93994
13.75502	0.86343	13.74271	0.61317	13.74795	0.70551	13.75391	0.81772	13.75793	0.94417
13.75588	0.89540	13.74286	0.60630	13.74880	0.70364	13.75406	0.82437		
13.75604	0.87846	13.74363	0.62629	13.74896	0.70936	13.75486	0.86899		
13.75680	0.91519	13.74378	0.63679	13.74972	0.72747	13.75502	0.86343		

V Observations

JD HEL. 2447670+	DELTA V MAG	JD HEL. 2447670+	DELTA V MAG	JD HEL. 2447670+	DELTA V MAG	JD HEL. 2447670+	DELTA V MAG	JD HEL. 2447670+	DELTA V MAG
7.70717	0.9974	8.76960	1.0933	9.68119	1.0360	9.71444	0.4697	9.74632	0.3673
7.70756	0.9752	8.77159	1.0318	9.68183	1.0184	9.71484	0.4715	9.74839	0.3650
7.70808	0.9699	8.77198	1.0230	9.68221	1.0171	9.71541	0.4673	9.74878	0.3641
7.70845	0.9724	8.77256	1.0101	9.68425	0.9536	9.71579	0.4813	9.74937	0.3665
7.71470	0.8145	8.77293	0.9966	9.68464	0.9320	9.71780	0.4640	9.74975	0.3520
7.71508	0.8033	8.77498	0.9287	9.68523	0.9446	9.71818	0.4434	9.75179	0.3596
7.71565	0.7933	8.77537	0.9295	9.68561	0.9255	9.71880	0.4536	9.75218	0.3900
7.71603	0.7877	8.77596	0.9120	9.68764	0.8757	9.71917	0.4483	9.75277	0.3817
7.71800	0.7609	8.77633	0.9164	9.68802	0.8647	9.72112	0.4092	9.75316	0.3857
7.71839	0.7537	8.77844	0.8349	9.68864	0.8353	9.72151	0.4472	9.75510	0.3847
7.71911	0.7633	8.77883	0.8194	9.68902	0.8367	9.72227	0.4275	9.75549	0.3930
7.71949	0.7672	8.77936	0.8138	9.69105	0.7748	9.72264	0.4117	9.75613	0.3975
7.72176	0.7371	8.77974	0.8053	9.69144	0.7607	9.72484	0.4155	9.75653	0.3831
7.72215	0.6939	8.78176	0.7582	9.69199	0.7419	9.72523	0.4202	9.75859	0.3945
7.72272	0.6874	8.78215	0.7417	9.69237	0.7501	9.72578	0.4103	9.75898	0.3781
7.72310	0.6893	8.78282	0.7317	9.69445	0.7174	9.72616	0.4302	9.75954	0.4082
7.72538	0.6630	8.78320	0.7138	9.69483	0.7089	9.72813	0.4285	9.75992	0.3846
7.72577	0.6599	8.78624	0.6616	9.69539	0.6992	9.72852	0.4195	9.76189	0.3789
7.72633	0.6513	8.78662	0.6804	9.69577	0.7020	9.72909	0.4082	9.76229	0.3909
7.72671	0.6309	8.78871	0.6382	9.69776	0.6547	9.72947	0.4099	9.76284	0.4056
7.72868	0.6242	8.78910	0.6347	9.69814	0.6511	9.73141	0.4030	9.76322	0.3786
7.72907	0.6127	8.78983	0.6011	9.69869	0.6434	9.73180	0.4024	9.76549	0.4161
7.72969	0.6016	8.79020	0.6061	9.69907	0.6280	9.73236	0.4133	9.76587	0.4188
7.73007	0.5990	9.66676	1.1983	9.70126	0.5937	9.73274	0.4045	9.76645	0.4120
7.73245	0.5604	9.66800	1.2165	9.70165	0.5925	9.73472	0.4109	9.76683	0.4210
7.73285	0.5678	9.66838	1.2010	9.70221	0.5855	9.73510	0.3987	9.76875	0.4274
7.73342	0.5865	9.67034	1.2038	9.70258	0.6072	9.73566	0.4001	9.76914	0.4349
7.73380	0.5854	9.67073	1.2079	9.70455	0.5333	9.73604	0.4084	9.76970	0.4313
8.76081	1.2162	9.67136	1.2001	9.70494	0.5235	9.73799	0.3853	9.77008	0.4347
8.76120	1.2244	9.67174	1.2209	9.70550	0.5128	9.73838	0.3682	9.77215	0.4331
8.76254	1.2098	9.67385	1.1981	9.70589	0.5282	9.73893	0.3738	9.77254	0.4455
8.76292	1.2214	9.67424	1.1953	9.70792	0.5225	9.73931	0.3877	9.77317	0.4361
8.76482	1.1893	9.67480	1.2108	9.70831	0.5056	9.74142	0.3582	9.77355	0.4489
8.76521	1.1608	9.67518	1.2067	9.70887	0.5146	9.74181	0.3633	9.77563	0.4639
8.76578	1.1938	9.67738	1.1528	9.70925	0.5110	9.74237	0.3524	9.77601	0.4735
8.76616	1.1687	9.67777	1.1530	9.71115	0.4978	9.74275	0.3712	9.77662	0.5037
8.76821	1.1248	9.67843	1.1189	9.71154	0.4898	9.74488	0.3780	9.77700	0.4722
8.76859	1.1115	9.67880	1.0907	9.71211	0.4826	9.74527	0.3800	9.77910	0.4652
8.76922	1.1092	9.68080	1.0423	9.71249	0.4812	9.74594	0.3776	9.77949	0.5226

TABLE 1. (continued)

JD HEL. 2447670+	DELTA V MAG	JD HEL. 2447670+	DELTA V MAG	JD HEL. 2447670+	DELTA V MAG	JD HEL. 2447670+	DELTA V MAG	JD HEL. 2447670+	DELTA V MAG
10.67512	0.4038	10.72042	0.9427	10.76834	0.5670	11.69645	0.4920	11.73834	0.5082
10.67550	0.4170	10.72232	0.9851	10.76873	0.5583	11.69710	0.4714	11.73860	0.4936
10.67611	0.4211	10.72272	0.9903	10.76933	0.5728	11.69736	0.4899	11.74049	0.4730
10.67648	0.4110	10.72332	1.0033	10.76970	0.5723	11.69995	0.4616	11.74076	0.5056
10.67836	0.4179	10.72370	1.0228	10.77676	0.5380	11.70022	0.4592	11.74138	0.4843
10.67875	0.4102	10.72563	1.0382	10.77715	0.5356	11.70080	0.4732	11.74164	0.4943
10.67934	0.4262	10.72602	1.0526	10.77770	0.5155	11.70107	0.4621	11.74276	0.5033
10.67972	0.4300	10.72658	1.0375	10.77808	0.5348	11.70168	0.4529	11.74302	0.5092
10.68168	0.4188	10.72696	1.0629	10.78002	0.5088	11.70195	0.4673	11.75007	0.4991
10.68207	0.4278	10.72881	1.0830	10.78041	0.5058	11.70386	0.4496	11.75035	0.5251
10.68265	0.4383	10.72919	1.0987	10.78100	0.4948	11.70414	0.4464	11.75112	0.4923
10.68303	0.4476	10.72979	1.0896	10.78137	0.4925	11.70478	0.4577	11.75139	0.5288
10.68495	0.4468	10.73017	1.0923	10.78351	0.4994	11.70504	0.4533	11.75202	0.5862
10.68534	0.4654	10.73210	1.1199	10.78390	0.4828	11.70569	0.4320	11.75228	0.5390
10.68593	0.4700	10.73249	1.1095	10.78454	0.4734	11.70596	0.4397	11.75434	0.6186
10.68631	0.4687	10.73309	1.1029	10.78492	0.4909	11.70796	0.4571	11.75461	0.5631
10.68832	0.4706	10.73346	1.0937	11.67095	0.6587	11.70823	0.4352	11.75522	0.5351
10.68870	0.4849	10.73532	1.0784	11.67122	0.6562	11.70882	0.4396	11.75548	0.5735
10.68926	0.4742	10.73571	1.0799	11.67182	0.6575	11.70909	0.4377	11.75615	0.5823
10.68964	0.4947	10.73628	1.0861	11.67208	0.6355	11.70972	0.4288	11.75642	0.5673
10.69156	0.5006	10.73666	1.0876	11.67276	0.6296	11.70998	0.4459	11.75841	0.5669
10.69195	0.4906	10.73860	1.0559	11.67302	0.6268	11.71191	0.4190	11.75869	0.5874
10.69255	0.5143	10.73899	1.0378	11.67495	0.6100	11.71218	0.4354	11.75930	0.5794
10.69293	0.5112	10.73953	1.0316	11.67522	0.6084	11.71277	0.4316	11.75957	0.5900
10.69486	0.5259	10.73991	1.0402	11.67582	0.5837	11.71304	0.4128	11.76031	0.5912
10.69524	0.5238	10.74177	0.9826	11.67609	0.5912	11.71374	0.4233	11.76057	0.5983
10.69606	0.5319	10.74215	0.9672	11.67680	0.5918	11.71401	0.4259	11.76260	0.6382
10.69643	0.5410	10.74268	0.9473	11.67706	0.5806	11.71593	0.4670	11.76287	0.6380
10.69852	0.5564	10.74307	0.9468	11.67902	0.5626	11.71621	0.4649	11.76354	0.6398
10.69891	0.5462	10.74497	0.8980	11.67929	0.5684	11.71707	0.4372	11.76381	0.6494
10.69983	0.5704	10.74536	0.8940	11.67992	0.5625	11.72005	0.4233	11.76443	0.6624
10.70021	0.5734	10.74596	0.9025	11.68018	0.5512	11.72033	0.4825	11.76470	0.6777
10.70228	0.5988	10.74634	0.8738	11.68088	0.5577	11.72098	0.4141	11.76670	0.7420
10.70267	0.5949	10.74829	0.8161	11.68114	0.5461	11.72124	0.4151	11.76698	0.7131
10.70326	0.6026	10.74868	0.8129	11.68323	0.5492	11.72188	0.4393	11.76760	0.7309
10.70364	0.6069	10.74930	0.7796	11.68350	0.5249	11.72215	0.4082	11.76787	0.7170
10.70569	0.6471	10.74967	0.7839	11.68411	0.5263	11.72445	0.4524	11.76850	0.7603
10.70608	0.6529	10.75161	0.7727	11.68437	0.5342	11.72505	0.4570	11.76877	0.7616
10.70669	0.6764	10.75200	0.7606	11.68502	0.5282	11.72532	0.4396	11.77083	0.8024
10.70706	0.6579	10.75256	0.7526	11.68528	0.5142	11.72599	0.4713	11.77110	0.8039
10.70898	0.7149	10.75294	0.7498	11.68729	0.5137	11.72625	0.4550	11.77173	0.8116
10.70937	0.7189	10.75486	0.7372	11.68756	0.5436	11.72856	0.5115	11.77200	0.8072
10.70997	0.7240	10.75524	0.7634	11.68825	0.4948	11.72919	0.4873	11.77264	0.8310
10.71035	0.7235	10.75587	0.7325	11.68851	0.5052	11.72946	0.4771	11.77290	0.8278
10.71231	0.7634	10.75624	0.7722	11.68912	0.5109	11.73009	0.4756	11.77489	0.9211
10.71270	0.7865	10.75825	0.7030	11.68938	0.4974	11.73035	0.4816	11.77516	0.9167
10.71342	0.7930	10.75864	0.6915	11.69135	0.5111	11.73248	0.5228	11.77606	0.9453
10.71380	0.8010	10.75926	0.6694	11.69163	0.5160	11.73276	0.4936	11.77673	0.9569
10.71581	0.8530	10.75964	0.6595	11.69225	0.5231	11.73339	0.4642	11.77700	0.9468
10.71620	0.8541	10.76256	0.6298	11.69251	0.5138	11.73365	0.4718	11.77898	0.9941
10.71675	0.8749	10.76294	0.6200	11.69311	0.4979	11.73429	0.4401	11.77925	1.0127
10.71713	0.8761	10.76493	0.6171	11.69338	0.5034	11.73455	0.4670	11.77987	1.0120
10.71906	0.9189	10.76533	0.5795	11.69528	0.4809	11.73649	0.4853	11.78014	1.0400
10.71946	0.9236	10.76586	0.5905	11.69555	0.4839	11.73676	0.5289	11.78081	1.0420
10.72004	0.9421	10.76623	0.6090	11.69619	0.4844	11.73769	0.4931	11.78107	1.0673

TABLE 1. (continued)

JD HEL. 2447670+	DELTA V MAG	JD HEL. 2447670+	DELTA V MAG	JD HEL. 2447670+	DELTA V MAG	JD HEL. 2447670+	DELTA V MAG	JD HEL. 2447670+	DELTA V MAG
11.78306	1.1135	13.73043	0.5523	13.73902	0.6101	13.74621	0.7427	13.75325	0.9069
11.78334	1.1245	13.73101	0.5601	13.73958	0.6189	13.74673	0.7625	13.75379	0.9115
11.78424	1.1575	13.73142	0.5439	13.73999	0.6427	13.74714	0.7465	13.75419	0.9021
11.78738	1.2037	13.73200	0.5651	13.74054	0.6510	13.74767	0.7774	13.75474	0.9236
11.78888	1.2118	13.73240	0.5542	13.74094	0.6482	13.74807	0.8016	13.75514	0.9389
13.72586	0.5037	13.73431	0.5837	13.74165	0.6523	13.74868	0.8026	13.75576	0.9466
13.72628	0.5118	13.73472	0.5852	13.74206	0.6747	13.74908	0.8123	13.75616	0.9278
13.72680	0.5187	13.73528	0.5831	13.74258	0.6822	13.74960	0.8128	13.75668	0.9512
13.72720	0.5282	13.73569	0.5940	13.74299	0.7018	13.75000	0.8211	13.75709	0.9814
13.72774	0.5191	13.73627	0.5935	13.74351	0.7206	13.75055	0.8367	13.75764	0.9943
13.72815	0.5314	13.73667	0.5802	13.74391	0.7107	13.75095	0.8309	13.75805	1.0026
13.73001	0.5458	13.73861	0.6215	13.74580	0.7364	13.75283	0.8802		

R Observations

JD HEL. 2447670+	DELTA R MAG	JD HEL. 2447670+	DELTA R MAG	JD HEL. 2447670+	DELTA R MAG	JD HEL. 2447670+	DELTA R MAG	JD HEL. 2447670+	DELTA R MAG
7.70709	1.0032	8.76607	1.1733	9.67415	1.1925	9.70485	0.5672	9.73558	0.4197
7.70747	0.9889	8.76812	1.1004	9.67472	1.1938	9.70542	0.5463	9.73595	0.4279
7.70799	0.9790	8.76851	1.1104	9.67509	1.1796	9.70580	0.5593	9.73790	0.4298
7.70837	0.9693	8.76913	1.0966	9.67729	1.1522	9.70783	0.5404	9.73829	0.4213
7.71461	0.8365	8.76951	1.0795	9.67769	1.1394	9.70822	0.5263	9.73884	0.4184
7.71500	0.8251	8.77151	1.0268	9.67834	1.1173	9.70878	0.5308	9.73922	0.4242
7.71556	0.8395	8.77190	1.0062	9.67872	1.1078	9.70916	0.5332	9.74133	0.4088
7.71594	0.8016	8.77247	1.0043	9.68072	1.0477	9.71107	0.5243	9.74173	0.3958
7.71792	0.7730	8.77285	0.9825	9.68111	1.0525	9.71145	0.5098	9.74228	0.4125
7.71830	0.7510	8.77489	0.9364	9.68174	1.0167	9.71202	0.5129	9.74266	0.4017
7.71902	0.7654	8.77529	0.9280	9.68212	1.0133	9.71240	0.5163	9.74479	0.4121
7.71940	0.7925	8.77587	0.9202	9.68417	0.9531	9.71435	0.5105	9.74518	0.3915
7.72167	0.7446	8.77624	0.9161	9.68456	0.9445	9.71475	0.5123	9.74586	0.4095
7.72206	0.7238	8.77836	0.8468	9.68514	0.9437	9.71532	0.5103	9.74623	0.4109
7.72264	0.7139	8.77875	0.8272	9.68552	0.9274	9.71570	0.5018	9.74831	0.4052
7.72302	0.7042	8.77928	0.8353	9.68755	0.8959	9.71771	0.4974	9.74869	0.4001
7.72530	0.6691	8.77965	0.8045	9.68794	0.8835	9.71809	0.4962	9.74928	0.3999
7.72568	0.6570	8.78167	0.7680	9.68854	0.8506	9.71871	0.4846	9.74966	0.4023
7.72625	0.6560	8.78206	0.7688	9.68893	0.8593	9.71909	0.4887	9.75170	0.4196
7.72662	0.6485	8.78273	0.7103	9.69096	0.8009	9.72142	0.4677	9.75209	0.4182
7.72859	0.6318	8.78311	0.7328	9.69135	0.7685	9.72218	0.4605	9.75268	0.4163
7.72898	0.6270	8.78616	0.6893	9.69190	0.7660	9.72256	0.4495	9.75307	0.4341
7.72960	0.6103	8.78653	0.6981	9.69228	0.7507	9.72476	0.4453	9.75501	0.4196
7.72998	0.6023	8.78863	0.6581	9.69436	0.7270	9.72515	0.4491	9.75541	0.4168
7.73237	0.5774	8.78901	0.6608	9.69475	0.7176	9.72570	0.4473	9.75602	0.4177
7.73276	0.5898	8.78974	0.6340	9.69530	0.7032	9.72608	0.4453	9.75644	0.4149
7.73333	0.5832	8.79011	0.6099	9.69568	0.7037	9.72804	0.4518	9.75850	0.4092
8.75663	1.1987	9.66667	1.1916	9.69767	0.6729	9.72843	0.4314	9.75889	0.4232
8.75799	1.1925	9.66706	1.2070	9.69806	0.6525	9.72900	0.4441	9.75946	0.4267
8.76073	1.2078	9.66791	1.2124	9.69861	0.6533	9.72938	0.4524	9.75983	0.4280
8.76111	1.2009	9.66829	1.2114	9.69898	0.6473	9.73133	0.4304	9.76181	0.4160
8.76245	1.1959	9.67026	1.2074	9.70117	0.6196	9.73172	0.4244	9.76220	0.4191
8.76283	1.1926	9.67064	1.1935	9.70156	0.6161	9.73227	0.4235	9.76276	0.4228
8.76473	1.1717	9.67127	1.1823	9.70212	0.6228	9.73265	0.4295	9.76314	0.4291
8.76512	1.1856	9.67165	1.2041	9.70250	0.6150	9.73463	0.4153	9.76540	0.4427
8.76569	1.1741	9.67376	1.2025	9.70447	0.5746	9.73502	0.4252	9.76579	0.4421

TABLE 1. (continued)

JD HEL. 2447670+	DELTA R MAG	JD HEL. 2447670+	DELTA R MAG	JD HEL. 2447670+	DELTA R MAG	JD HEL. 2447670+	DELTA R MAG	JD HEL. 2447670+	DELTA R MAG
9.76637	0.4603	10.70928	0.7229	10.75516	0.7446	11.68903	0.5383	11.73000	0.5120
9.76674	0.4505	10.70988	0.7329	10.75578	0.7460	11.68947	0.5256	11.73044	0.4892
9.76866	0.4469	10.71026	0.7601	10.75616	0.7228	11.69126	0.5415	11.73239	0.5398
9.76905	0.4609	10.71223	0.7770	10.75817	0.6890	11.69171	0.5240	11.73284	0.4813
9.76962	0.4558	10.71261	0.7919	10.75855	0.6731	11.69216	0.5398	11.73330	0.4694
9.76999	0.4615	10.71334	0.8115	10.75917	0.6686	11.69260	0.5251	11.73374	0.4964
9.77207	0.4426	10.71371	0.8161	10.75955	0.6566	11.69303	0.5233	11.73420	0.4564
9.77308	0.4333	10.71572	0.8560	10.76186	0.6766	11.69346	0.5225	11.73464	0.4703
9.77346	0.4646	10.71611	0.8702	10.76248	0.6276	11.69519	0.5069	11.73640	0.4663
9.77554	0.4814	10.71667	0.8922	10.76285	0.6201	11.69564	0.5163	11.73686	0.5121
9.77593	0.4936	10.71704	0.8927	10.76485	0.6112	11.69610	0.5040	11.73734	0.4654
9.77653	0.5098	10.71898	0.8860	10.76524	0.6045	11.69654	0.5038	11.73778	0.4791
9.77691	0.5058	10.71937	0.9389	10.76577	0.6168	11.69701	0.5102	11.73825	0.4795
9.77901	0.5208	10.71996	0.9299	10.76615	0.6360	11.69745	0.5145	11.73869	0.4810
9.77941	0.5347	10.72034	0.9462	10.76825	0.5797	11.69985	0.4910	11.74040	0.4739
10.67503	0.4455	10.72224	0.9883	10.76864	0.5899	11.70031	0.4838	11.74085	0.4787
10.67541	0.4455	10.72263	1.0003	10.76924	0.5777	11.70072	0.4943	11.74129	0.4819
10.67602	0.4475	10.72323	1.0054	10.76962	0.5801	11.70115	0.4811	11.74173	0.4980
10.67640	0.4384	10.72361	1.0265	10.77667	0.5401	11.70160	0.4797	11.74267	0.5138
10.67828	0.4518	10.72554	1.0585	10.77706	0.5301	11.70203	0.4789	11.74311	0.5452
10.67867	0.4595	10.72593	1.0721	10.77761	0.5465	11.70378	0.4770	11.74999	0.5504
10.67925	0.4723	10.72649	1.0493	10.77799	0.5305	11.70423	0.4737	11.75044	0.5520
10.67963	0.4635	10.72687	1.0505	10.77993	0.5353	11.70469	0.4758	11.75104	0.5282
10.68159	0.4602	10.72872	1.0829	10.78128	0.5327	11.70513	0.4728	11.75147	0.5789
10.68198	0.4722	10.72910	1.0854	10.78342	0.5095	11.70561	0.4688	11.75193	0.5923
10.68256	0.4825	10.72971	1.0958	10.78381	0.5040	11.70605	0.4686	11.75237	0.5841
10.68294	0.4744	10.73008	1.1210	10.78445	0.4900	11.70787	0.4690	11.75425	0.5861
10.68486	0.4862	10.73202	1.1125	10.78483	0.4891	11.70832	0.4600	11.75470	0.5923
10.68525	0.4908	10.73241	1.1131	11.67086	0.6867	11.70873	0.4577	11.75513	0.5901
10.68585	0.4919	10.73300	1.1099	11.67130	0.6698	11.70918	0.4638	11.75557	0.6195
10.68622	0.4907	10.73337	1.1020	11.67173	0.6796	11.70963	0.4802	11.75606	0.5933
10.68823	0.4969	10.73524	1.0698	11.67217	0.6685	11.71007	0.5000	11.75650	0.6273
10.68862	0.5008	10.73562	1.0804	11.67267	0.6648	11.71182	0.4510	11.75832	0.5958
10.68918	0.5062	10.73619	1.0844	11.67311	0.6465	11.71227	0.4648	11.75877	0.6373
10.68955	0.5055	10.73657	1.0831	11.67486	0.6278	11.71268	0.4637	11.75922	0.6137
10.69148	0.5155	10.73851	1.0464	11.67531	0.6103	11.71313	0.4422	11.75966	0.6152
10.69186	0.5134	10.73890	1.0412	11.67574	0.6033	11.71366	0.4568	11.76022	0.6192
10.69246	0.5289	10.73944	1.0424	11.67617	0.6207	11.71409	0.4508	11.76066	0.6033
10.69284	0.5279	10.73982	1.0172	11.67671	0.6121	11.71585	0.4793	11.76252	0.6607
10.69477	0.5476	10.74168	0.9844	11.67715	0.6026	11.71630	0.4711	11.76296	0.6533
10.69516	0.5518	10.74207	0.9785	11.67893	0.5946	11.71716	0.4568	11.76346	0.6617
10.69597	0.5583	10.74259	0.9565	11.67938	0.5945	11.71996	0.4402	11.76390	0.6644
10.69635	0.5609	10.74298	0.9633	11.67983	0.5884	11.72041	0.4563	11.76435	0.6522
10.69843	0.5807	10.74489	0.9143	11.68027	0.5692	11.72089	0.4414	11.76661	0.7395
10.69882	0.5887	10.74527	0.9096	11.68079	0.5680	11.72133	0.4446	11.76706	0.7603
10.69974	0.5872	10.74587	0.9008	11.68123	0.5642	11.72180	0.4565	11.76751	0.7487
10.70012	0.5888	10.74625	0.8997	11.68314	0.5624	11.72223	0.4367	11.76795	0.7509
10.70219	0.6247	10.74820	0.8468	11.68359	0.5435	11.72454	0.4800	11.76842	0.7509
10.70258	0.6203	10.74860	0.8370	11.68402	0.5438	11.72496	0.4953	11.76886	0.7639
10.70317	0.6221	10.74921	0.7829	11.68446	0.5380	11.72540	0.4798	11.77075	0.8055
10.70355	0.6191	10.74959	0.8006	11.68493	0.5480	11.72590	0.4797	11.77119	0.8118
10.70560	0.6619	10.75152	0.7690	11.68537	0.5344	11.72634	0.4791	11.77165	0.8480
10.70599	0.6551	10.75191	0.7734	11.68720	0.5362	11.72819	0.5139	11.77209	0.8467
10.70660	0.6748	10.75247	0.7822	11.68765	0.5461	11.72865	0.5106	11.77255	0.8695
10.70697	0.6694	10.75285	0.7610	11.68816	0.5220	11.72910	0.4915	11.77299	0.8684
10.70889	0.7188	10.75477	0.7523	11.68860	0.5231	11.72954	0.4874	11.77480	0.9165

TABLE 1. (continued)

JD HEL. 2447670+	DELTA R MAG	JD HEL. 2447670+	DELTA R MAG	JD HEL. 2447670+	DELTA R MAG	JD HEL. 2447670+	DELTA R MAG	JD HEL. 2447670+	DELTA R MAG
11.77525	0.9031	13.72767	0.5405	13.74251	0.7099	13.75568	0.9537	13.77221	1.0597
11.77570	0.9327	13.72822	0.5545	13.74306	0.7319	13.75624	0.9887	13.77362	1.0113
11.77615	0.9527	13.72993	0.5664	13.74343	0.7268	13.75661	0.9806	13.77417	1.0518
11.77665	0.9193	13.73050	0.5513	13.74399	0.7327	13.75716	0.9913	13.77455	1.0241
11.77709	0.9571	13.73093	0.5567	13.74572	0.7890	13.75757	1.0080	13.77690	0.9201
11.77889	0.9739	13.73149	0.5586	13.74629	0.7890	13.75813	1.0193	13.77747	0.9205
11.77934	0.9998	13.73192	0.5693	13.74666	0.7947	13.76082	1.0746	13.77784	0.9244
11.77979	1.0212	13.73248	0.5685	13.74721	0.8009	13.76137	1.0615	13.77840	0.9257
11.78023	1.0502	13.73423	0.5667	13.74759	0.8153	13.76181	1.0928	13.77878	0.9287
11.78072	1.0871	13.73480	0.5828	13.74815	0.8345	13.76237	1.0731	13.78100	0.8552
11.78116	1.0536	13.73521	0.6048	13.74860	0.8132	13.76280	1.0696	13.78157	0.8618
11.78297	1.1058	13.73576	0.6053	13.74916	0.8328	13.76336	1.0993	13.78192	0.8926
11.78389	1.1087	13.73619	0.6113	13.74953	0.8294	13.76426	1.0754	13.78247	0.8949
11.78433	1.1329	13.73675	0.6135	13.75008	0.8360	13.76525	1.0834	13.78288	0.7886
11.78343	1.1273	13.73853	0.6477	13.75047	0.8429	13.76561	1.0938	13.78343	0.8405
11.78485	1.1821	13.73910	0.6460	13.75102	0.8755	13.76616	1.0628	13.78388	0.8234
11.78529	1.1784	13.73951	0.6532	13.75276	0.8827	13.76656	1.0862	13.78444	0.8608
11.78835	1.2073	13.74007	0.6564	13.75332	0.9618	13.76712	1.0818	13.78484	0.7689
13.72578	0.5236	13.74046	0.6910	13.75371	0.9161	13.76980	1.0573	13.78577	0.7860
13.72635	0.5472	13.74102	0.6864	13.75426	0.9179	13.77037	1.0694	13.78632	0.7824
13.72672	0.5443	13.74157	0.6980	13.75466	0.9465	13.77129	1.0676	13.78883	0.7318
13.72728	0.5548	13.74213	0.7099	13.75522	0.9599	13.77166	1.0814	13.78975	0.7277

I Observations

JD HEL. 2447670+	DELTA I MAG	JD HEL. 2447670+	DELTA I MAG	JD HEL. 2447670+	DELTA I MAG	JD HEL. 2447670+	DELTA I MAG	JD HEL. 2447670+	DELTA I MAG
7.70700	0.9723	7.73228	0.5867	8.77616	0.8812	9.67406	1.1547	9.69466	0.7267
7.70739	0.9653	7.73267	0.5957	8.77827	0.8220	9.67463	1.1475	9.69521	0.7034
7.70790	0.9409	7.73325	0.5927	8.77866	0.8095	9.67500	1.1499	9.69559	0.6960
7.70828	0.9516	8.75655	1.1356	8.77919	0.7926	9.67721	1.1178	9.69758	0.6519
7.71452	0.8276	8.75791	1.2059	8.77957	0.7942	9.67759	1.0963	9.69797	0.6576
7.71491	0.8333	8.76064	1.1547	8.78159	0.7655	9.67825	1.0713	9.69852	0.6392
7.71547	0.8064	8.76103	1.2066	8.78197	0.7930	9.67863	1.0610	9.69890	0.6376
7.71585	0.8045	8.76236	1.1778	8.78264	0.7258	9.68063	1.0256	9.70109	0.6128
7.71783	0.7748	8.76274	1.1269	8.78302	0.7395	9.68102	1.0248	9.70147	0.6100
7.71822	0.7681	8.76464	1.1312	8.78607	0.7035	9.68166	0.9995	9.70203	0.5974
7.71894	0.7548	8.76503	1.1188	8.78645	0.6972	9.68203	0.9862	9.70241	0.6105
7.71931	0.7719	8.76560	1.1280	8.78854	0.6509	9.68408	0.9334	9.70438	0.5685
7.72158	0.7074	8.76598	1.1237	8.78893	0.6384	9.68447	0.9310	9.70477	0.5599
7.72197	0.7210	8.76803	1.0713	8.78965	0.6400	9.68505	0.9281	9.70533	0.5558
7.72255	0.6972	8.76842	1.0617	8.79003	0.6276	9.68543	0.9048	9.70571	0.5520
7.72293	0.7027	8.76904	1.0616	9.66658	1.1778	9.68746	0.8612	9.70775	0.5519
7.72521	0.6690	8.76942	1.0541	9.66697	1.1643	9.68785	0.8667	9.70813	0.5446
7.72560	0.6630	8.77142	0.9797	9.66783	1.1627	9.68846	0.8491	9.70870	0.5336
7.72616	0.6514	8.77181	0.9869	9.66821	1.1303	9.68884	0.8343	9.70907	0.5463
7.72653	0.6488	8.77238	0.9832	9.67017	1.1720	9.69087	0.7922	9.71098	0.5274
7.72850	0.6201	8.77276	0.9555	9.67056	1.1810	9.69127	0.7801	9.71137	0.5299
7.72889	0.6275	8.77481	0.9008	9.67118	1.1611	9.69182	0.7680	9.71194	0.5301
7.72952	0.6150	8.77520	0.9204	9.67156	1.1670	9.69219	0.7637	9.71231	0.5103
7.72990	0.6157	8.77578	0.8878	9.67367	1.1658	9.69427	0.7429	9.71427	0.5106

TABLE 1. (continued)

JD HEL. 2447670+	DELTA I MAG	JD HEL. 2447670+	DELTA I MAG	JD HEL. 2447670+	DELTA I MAG	JD HEL. 2447670+	DELTA I MAG	JD HEL. 2447670+	DELTA I MAG
9.71466	0.5054	9.75937	0.4265	10.69873	0.5887	10.74198	0.9583	11.67565	0.6187
9.71523	0.4975	9.75974	0.4310	10.69966	0.5875	10.74251	0.9476	11.67626	0.6062
9.71561	0.5033	9.76172	0.4380	10.70003	0.5912	10.74289	0.9458	11.67662	0.6093
9.71762	0.5125	9.76211	0.4396	10.70211	0.6346	10.74480	0.9036	11.67724	0.5988
9.71801	0.4845	9.76267	0.4506	10.70249	0.6240	10.74519	0.8979	11.67885	0.5829
9.71862	0.4897	9.76305	0.4374	10.70308	0.6235	10.74579	0.8957	11.67947	0.5733
9.71900	0.4841	9.76531	0.4517	10.70346	0.6367	10.74616	0.8827	11.67975	0.5783
9.72133	0.4808	9.76570	0.4520	10.70551	0.6593	10.74812	0.8428	11.68036	0.5771
9.72209	0.4597	9.76628	0.4479	10.70590	0.6650	10.74851	0.7636	11.68070	0.5611
9.72247	0.4579	9.76666	0.4332	10.70651	0.6741	10.74912	0.7789	11.68132	0.5562
9.72467	0.4558	9.76857	0.4375	10.70689	0.6744	10.74950	0.8219	11.68305	0.5665
9.72506	0.4490	9.76896	0.4706	10.70881	0.7176	10.75144	0.7903	11.68367	0.5469
9.72561	0.4644	9.76953	0.4649	10.70919	0.7204	10.75182	0.7735	11.68393	0.5617
9.72599	0.4743	9.76990	0.4714	10.70980	0.7309	10.75239	0.7842	11.68455	0.5495
9.72795	0.4655	9.77198	0.4701	10.71017	0.7365	10.75277	0.7629	11.68484	0.5482
9.72834	0.4664	9.77299	0.4810	10.71214	0.7684	10.75468	0.7614	11.68545	0.5386
9.72891	0.4686	9.77337	0.4620	10.71253	0.7925	10.75507	0.7544	11.68711	0.5474
9.72929	0.4538	9.77545	0.5061	10.71325	0.7915	10.75569	0.7364	11.68774	0.5541
9.73124	0.4513	9.77584	0.5279	10.71362	0.7968	10.75607	0.7303	11.68808	0.5346
9.73163	0.4541	9.77644	0.5130	10.71564	0.8641	10.75808	0.6768	11.68869	0.5204
9.73218	0.4433	9.77682	0.5232	10.71603	0.8679	10.75847	0.6785	11.68894	0.5281
9.73256	0.4434	9.77892	0.5138	10.71658	0.8860	10.75908	0.6698	11.68956	0.5287
9.73455	0.4315	9.77931	0.5424	10.71696	0.8766	10.75946	0.6592	11.69118	0.5418
9.73493	0.4410	10.67494	0.4544	10.71889	0.8264	10.76178	0.7147	11.69180	0.5297
9.73549	0.4400	10.67533	0.4500	10.71928	0.9359	10.76239	0.6307	11.69208	0.5476
9.73586	0.4372	10.67593	0.4527	10.71987	0.9394	10.76276	0.6201	11.69269	0.5429
9.73782	0.4263	10.67631	0.4613	10.72025	0.9399	10.76476	0.5920	11.69293	0.5288
9.73820	0.4151	10.67819	0.4652	10.72215	0.9956	10.76515	0.5915	11.69355	0.5319
9.73875	0.4230	10.67858	0.4762	10.72254	0.9976	10.76568	0.6181	11.69510	0.5144
9.73913	0.4351	10.67917	0.4766	10.72314	1.0076	10.76606	0.5935	11.69573	0.5105
9.74125	0.4038	10.67955	0.4665	10.72352	1.0197	10.76817	0.5693	11.69601	0.5232
9.74164	0.4242	10.68151	0.4758	10.72545	1.0348	10.76855	0.5878	11.69663	0.5138
9.74220	0.3962	10.68189	0.4680	10.72584	1.0232	10.76915	0.5840	11.69692	0.5117
9.74258	0.4199	10.68248	0.4717	10.72641	1.0512	10.76953	0.5763	11.69753	0.5117
9.74470	0.4231	10.68285	0.4800	10.72678	1.0395	10.77658	0.5350	11.69977	0.4774
9.74509	0.4169	10.68477	0.4934	10.72863	1.0497	10.77697	0.5455	11.70039	0.4730
9.74577	0.4047	10.68516	0.4745	10.72902	1.0703	10.77752	0.5373	11.70063	0.4744
9.74614	0.4024	10.68575	0.4882	10.72962	1.0625	10.77790	0.5258	11.70124	0.4690
9.74822	0.4137	10.68613	0.4933	10.72999	1.0985	10.77984	0.5251	11.70151	0.4834
9.74861	0.4166	10.68814	0.5025	10.73193	1.0742	10.78120	0.5307	11.70212	0.4703
9.74920	0.4097	10.68853	0.5003	10.73232	1.0767	10.78333	0.5201	11.70368	0.4799
9.74957	0.3922	10.68909	0.5046	10.73291	1.0708	10.78372	0.5100	11.70431	0.4968
9.75162	0.4163	10.68947	0.5048	10.73329	1.0625	10.78436	0.5080	11.70460	0.4746
9.75200	0.4191	10.69138	0.5095	10.73515	1.0540	10.78474	0.5178	11.70522	0.4816
9.75260	0.4350	10.69177	0.5285	10.73554	1.0542	11.67077	0.6703	11.70552	0.4829
9.75298	0.4175	10.69238	0.5247	10.73610	1.0348	11.67139	0.6773	11.70613	0.4719
9.75493	0.4103	10.69276	0.5321	10.73648	1.0500	11.67164	0.6767	11.70778	0.4814
9.75532	0.4337	10.69468	0.5445	10.73842	1.0281	11.67225	0.6514	11.70841	0.4661
9.75591	0.4310	10.69507	0.5442	10.73881	1.0180	11.67259	0.6592	11.70864	0.4745
9.75636	0.4414	10.69588	0.5532	10.73936	1.0142	11.67320	0.6408	11.70926	0.4757
9.75841	0.4342	10.69626	0.5551	10.73973	0.9818	11.67477	0.6195	11.70955	0.4851
9.75880	0.4314	10.69834	0.5753	10.74159	0.9673	11.67540	0.6114	11.71016	0.4573

TABLE 1. (continued)

JD HEL. 2447670+	DELTA I MAG	JD HEL. 2447670+	DELTA I MAG	JD HEL. 2447670+	DELTA I MAG	JD HEL. 2447670+	DELTA I MAG	JD HEL. 2447670+	DELTA I MAG
11.71173	0.4594	11.74032	0.5231	11.77217	0.8310	13.73613	0.6011	13.76075	1.0920
11.71236	0.4617	11.74094	0.5148	11.77246	0.8384	13.73681	0.6118	13.76144	1.0561
11.71260	0.4696	11.74120	0.5329	11.77308	0.8411	13.73846	0.6328	13.76175	1.0484
11.71321	0.4482	11.74181	0.5184	11.77471	0.8835	13.73916	0.6553	13.76243	1.0405
11.71357	0.4653	11.74258	0.5468	11.77534	0.8919	13.73944	0.6290	13.76274	1.0440
11.71418	0.4845	11.74319	0.5493	11.77562	0.9475	13.74013	0.6705	13.76342	1.0540
11.71576	0.5135	11.74990	0.5441	11.77623	0.9068	13.74039	0.6731	13.76433	1.0755
11.71639	0.4780	11.75053	0.5522	11.77656	0.9020	13.74108	0.6806	13.76532	1.0529
11.71724	0.4764	11.75095	0.5461	11.77717	0.9636	13.74151	0.7004	13.76554	1.0659
11.71988	0.4565	11.75156	0.5781	11.77880	0.9642	13.74220	0.6992	13.76622	1.0666
11.72050	0.4595	11.75184	0.5630	11.77943	0.9939	13.74244	0.7100	13.76649	1.0751
11.72080	0.4525	11.75245	0.5647	11.77970	0.9921	13.74313	0.7069	13.76718	1.0745
11.72142	0.4548	11.75416	0.5831	11.78031	1.0125	13.74635	0.7844	13.77160	1.0225
11.72171	0.4625	11.75479	0.5905	11.78125	1.0410	13.74659	0.7784	13.77227	1.0340
11.72232	0.4646	11.75504	0.6051	11.78441	1.1440	13.74728	0.7901	13.77355	1.0298
11.72462	0.5004	11.75565	0.6148	11.78351	1.1037	13.74753	0.7946	13.77424	0.9970
11.72487	0.4906	11.75597	0.5820	11.78476	1.1979	13.74821	0.8018	13.77449	0.9749
11.72549	0.4922	11.75659	0.5912	11.78538	1.1106	13.74854	0.8270	13.77684	0.9034
11.72581	0.4694	11.75824	0.6141	11.78844	1.1494	13.74922	0.8448	13.77753	0.9057
11.72643	0.4790	11.75886	0.6221	13.72572	0.5497	13.74946	0.8322	13.77777	0.9085
11.72811	0.4470	11.75913	0.6405	13.72641	0.5450	13.75014	0.8508	13.77846	0.9445
11.72874	0.4913	11.75974	0.6374	13.72666	0.5517	13.75041	0.8502	13.77872	0.8785
11.72902	0.5014	11.76013	0.6338	13.72734	0.5559	13.75109	0.8562	13.78094	0.8593
11.72963	0.4665	11.76075	0.6396	13.72760	0.5587	13.75269	0.9093	13.78163	0.7942
11.72991	0.5046	11.76242	0.6541	13.72829	0.5496	13.75339	0.9401	13.78185	0.8216
11.73052	0.4870	11.76305	0.6651	13.72987	0.5708	13.75364	0.9191	13.78254	0.8729
11.73231	0.4985	11.76337	0.6691	13.73056	0.5731	13.75433	0.9324	13.78281	0.7606
11.73293	0.4813	11.76398	0.6726	13.73087	0.5751	13.75460	0.9318	13.78349	0.7629
11.73321	0.4832	11.76425	0.6925	13.73156	0.5623	13.75528	0.9297	13.78382	0.7780
11.73382	0.4769	11.76652	0.7116	13.73186	0.5940	13.75562	0.9662	13.78450	0.8181
11.73411	0.4788	11.76715	0.7269	13.73254	0.5708	13.75630	0.9337	13.78477	0.8156
11.73473	0.4870	11.76743	0.7481	13.73416	0.6011	13.75654	0.9811	13.78570	0.7473
11.73631	0.5130	11.76804	0.7284	13.73486	0.5958	13.75722	1.0077	13.78890	0.7183
11.73694	0.5485	11.76833	0.7439	13.73514	0.5889	13.75750	0.9969	13.78981	0.7823
11.73725	0.5078	11.76895	0.7526	13.73583	0.6106	13.75819	1.0062		
11.73787	0.5339	11.77066	0.8039	13.74336	0.7332	13.76974	1.0495		
11.73816	0.5105	11.77128	0.8238	13.74405	0.7386	13.77044	1.0453		
11.73878	0.5067	11.77156	0.8428	13.74565	0.7749	13.77136	1.0255		

(V) spectral range]. In the period–color plane for W UMa variables, CE Leo falls in the middle of the range found by Eggen (1967) and thus is typical of the cooler contact systems which he surveyed. The standard magnitudes of CE Leo during what we assume to be the unspotted (immaculate) maximum, i.e., Max II, and the flux ratio of the components indicates that the primary and the secondary component have V magnitudes of $12^{m}.52$ and $12^{m}.91$, respectively.

TABLE 2. Standard magnitudes of CE Leonis, comparison, and check stars.

Star	V	B-V	V-Rc	Rc-Ic	V-Ic	Phase
Comparison	11.507(15)	0.977(8)	0.533(7)	0.306(8)	0.839(9)	-
Check	12.210(28)	0.570(9)	0.355(3)	0.176(11)	0.531(18)	-
Variable	12.748(33)	0.943(13)	0.543(4)	0.341(3)	0.881(1)	0.00
	11.877(7)	0.871(13)	0.505(6)	0.283(7)	0.788(8)	0.25
	12.524(23)	0.925(7)	0.530(9)	0.339(14)	0.869(19)	0.50
	11.947(3)	0.882(2)	0.498(3)	0.297(2)	0.795(1)	0.75

4. PERIOD ANALYSIS

Three epochs of minimum light were determined from *BVRI* observations made during one primary and two secondary eclipses. An iterative technique based on the method of Hertzsprung (1928) was used for the first two, and the bisection of chords technique for the third. Our epochs of minimum light are given in Table 3 as means of times in the four bandpasses along with all other timings found in the literature. The visual timings found in the earlier B.B.S.A.G. bulletins #9–#37 were not used in our analysis because their large scatter tended to mask the period behavior suggested by the rest of the data. Here, we have corrected the time of minimum given by Samec & Bookmyer (1987a), which mistakenly had been taken as a primary minimum, was in error by one Julian day, and for which the heliocentric correction had been miscalculated. These data cover 28 years of observation or about 33 000 orbital revolutions. Since period changes in W UMa bina-

TABLE 3. Epochs of minimum light, CE Leonis.

JD Hel. 2448000+	Minimum	Cycles	$(O-C)_1$	$(O-C)_2$	Source
37651.642	I	-33049.0	-0.0043	-0.0400	MW
37737.528	I	-32766.0	0.0109	-0.0240	MW
38111.500	II	-31533.5	0.0056	-0.0268	MW
38112.410	II	-31530.5	0.0049	-0.0271	MW
38112.560	I	-31530.0	0.0031	-0.0288	MW
38113.470	I	-31527.0	0.0029	-0.0291	MW
38113.620	II	-31526.5	0.0011	-0.0308	MW
38116.340	II	-31517.5	-0.0097	-0.0417	MW
38116.500	I	-31517.0	-0.0014	-0.0334	MW
38134.412	I	-31458.0	0.0082	-0.0236	MW
38412.650	I	-30541.0	0.0007	-0.0290	MW
38414.610	II	-30534.5	-0.0116	-0.0413	MW
38415.690	I	-30531.0	0.0064	-0.0233	MW
38446.620	I	-30429.0	-0.0134	-0.0429	MW
38457.402	II	-30393.5	-0.0032	-0.0325	MW
38458.315	II	-30390.5	-0.0005	-0.0299	MW
38463.480	II	-31373.5	0 0061	-0.0231	MW
38463.620	I	-31373.0	-0.0055	-0.0349	MW
38464.390	II	-30370.5	0.0059	-0.0234	MW
38464.540	I	-30370.0	0.0042	-0.0251	MW
38465.450	I	-30367.0	0.0039	-0.0254	MW
38466.340	I	-30364.0	-0.0164	-0.0457	MW
45044.5495	II	-8684.5	0.0002	-0.0002	HO
45047.4325	I	-8675.0	0.0006	0.0002	HO
46929.0089	II	-2803.5	-0.0006	0.0000	SA
47655.402	I	-80.0	0.0071	0.0074	BB
47679.6687	I	0.0	-0.0004	-0.0002	PO
47680.7320	II	3.5	0.0009	0.0011	PO
47683.7642	II	13.5	-0.0011	-0.0009	PO

Note: MW = Meinunger & Wenzel (1968), HO = Hoffman (1983), SA = Samec and Bookmyer (1987), BB = BBSAG #92 (1989), PO = Present Observations

ries are usually discernible after about ten years of observations, we expected to see some period variation.

To calculate an ephemeris that most correctly represents the system at present, we fit the photoelectric epochs in Table 3 by a linear least squares with equal weights. We used our primary epoch and the period of Meinunger & Wenzel (1968) to assign cycle numbers, and obtained

$$\text{JD (hel.)Min I} = 2447679^{d}6689(3) + 0.30342785(5) \cdot E, \quad (2)$$

which was used to phase our observations in this paper. The O–C residuals calculated with this ephemeris (2) are shown graphically in Fig. 2 and are listed as $(O-C)_2$ in Table 3.

The uncertainty in the period defined by the early timings of Meinunger & Wenzell (1968) is sufficiently great that we cannot know for a fact whether the period at that epoch was less than, equal to, or greater than the period at the present epoch. The large gap between Meinunger–Wenzen and Hoffmann makes a definitive interpretation of any period variability impossible. The position of the O–C residuals in Fig. 2, however, indicates that, in the simplest interpretation, a period decrease (whether abrupt or continuous) must have occurred.

The size of such a minimum-required decrease, if abrupt, would have been $dP/P = -5.0\times10^{-6}$. This is in line with sizes of alternating period changes observed in many other W UMa binaries (Kreiner 1977) as well as in most binaries of other types containing at least one convective star (Tout & Hall 1991; Hall 1990). The current thinking is that such period changes, i.e., decreases and increases in the same binary alternating on a time scale of decades, result from magnetic cycles in a star with an active dynamo (Hall 1991).

The size of such a minimum-required period decrease, if continuous, can be estimated by fitting all of the times in Table 3 with a quadratic ephemeris. With the photoelectric timings weighted 1.0 and all others 0.01, the result was

$$\text{JD (hel.) Min I} = 2447679^{d}6690 \underset{\pm 8}{} + 0.3034275 \underset{\pm 2}{} \cdot E - 0.84\times10^{-10} \underset{\pm 12}{} \cdot E^2. \quad (3)$$

Residuals computed from ephemeris (3) are shown graphically in Fig. 3 and are listed as $(O-C)_1$ in Table 3. From the quadratic fit, which is statistically significant, we estimate $dP/dT = -1.0\times10^{-7}$ d/yr. A continuous period decrease may be due to angular momentum loss (AML) caused by stellar wind, i.e., ions spiralling away from the stars along corotating dynamo-induced magnetic field lines. Similar values of dP/dT have been found in other, similar W UMa binaries. For BX Peg (Samec 1990), V502 Oph (Derman & Demircan 1992), VW Cep (Lloyd *et al.* 1992, corrected for light-time due to the third body), V1010 Oph (Lipari & Sistero 1987), and EZ Hya (Lipari & Sistero 1987), the corresponding values are -1.4×10^{-7} d/yr, -2.1×10^{-7} d/yr, -2.0×10^{-7} d/yr, -4.1×10^{-7} d/yr, and -6.9×10^{-7} d/yr, respectively. The nature of the period behavior in EZ Hya is not conclusive due to its relatively short 17-year (14 000 cycles) observing span.

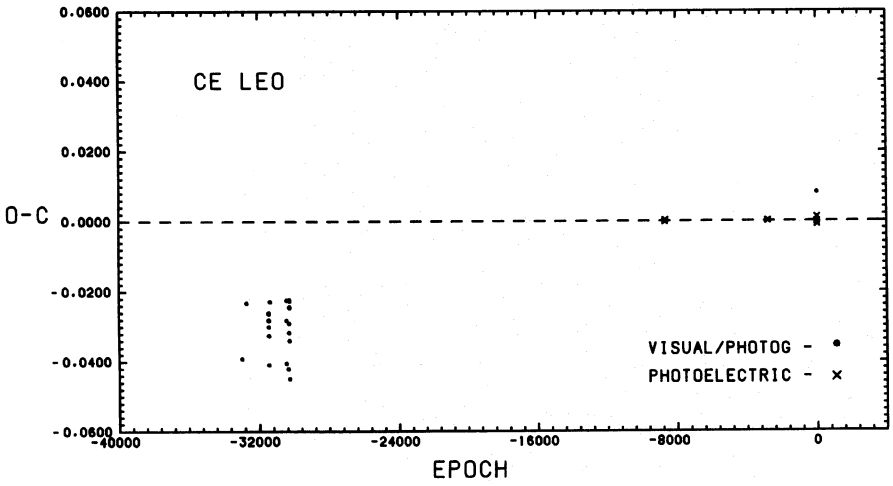

FIG. 2. Period behavior of CE Leo indicated by all available data calculated from Eq. (2).

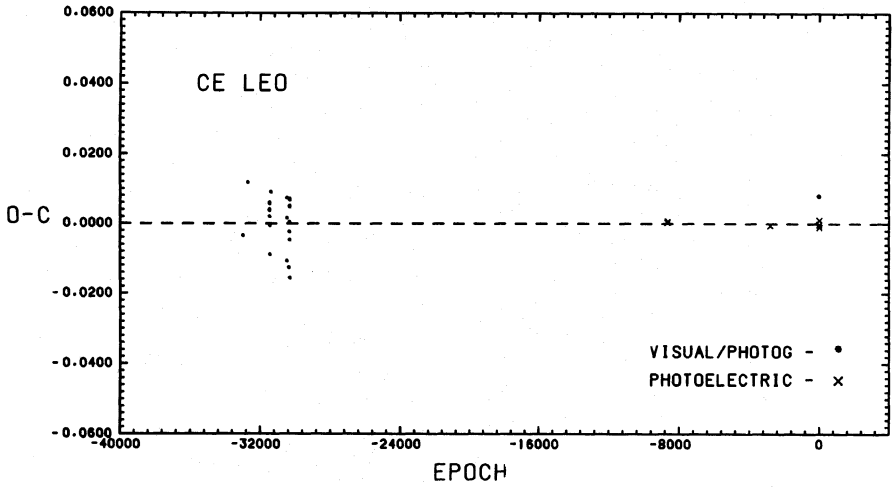

FIG. 3. O–C residuals of CE Leo determined from Eq. (3) for all available timings of minimum light.

Also, some of the period change in V1010 Oph may be ascribed to mass transfer from the primary, more massive component to the secondary since the thermal decoupling of the components implies semidetached state.

The quadratic fit in our Eq. (3) actually is somewhat poorer than one which could be achieved with linear fits, i.e., ones involving two abrupt period changes, an increase followed by a decrease, both of similar size (see Figs. 2 and 3). The previously mentioned unfortunate gap and the relatively small number of photoelectric timings, however, make the nature of its period changes not conclusive at this time. Since the nature of period variations in systems of this type are very important to our understanding of binary evolution, we invite observers to patrol this system over the next few decades or so. Also, searches of archived photographic plate material would be productive in this regard.

5. LIGHT CURVES

The B, V, R, and I light curves of CE Leo defined by the individual observations are plotted in Fig. 4 as Δm vs phase computed from the linear ephemeris in Eq. (2). The probable error for a single observation in B, V, R, and I is $\pm 0^{m}.012$, $\pm 0^{m}.008$, $\pm 0^{m}.009$, and $\pm 0^{m}.010$, respectively, so, 1% photometry was realized for the most part.

The light curves are typical of W UMa contact systems exhibiting a continual change in light output in the out-of-eclipse portion of the orbital cycle. A brief interval of constant light is discernible in the primary eclipse, particularly in the V and R normal point light curves in Fig. 5. This indicates that CE Leo is of W-type with the primary, more massive component being the cooler star. In this paper, parameters accompanied by an Arabic subscript 1 (primary component) refer to the larger, more massive, cooler component and parameters having a subscript 2 (secondary component) refer to the smaller, less massive, hotter component. The duration of totality as determined from our light curve solution found in the next section, is 20.0 min. Typical of highly distorted systems of this type, the $\Delta(B-V)$, and $\Delta(R-I)$ color curves are redder in the eclipses due to gravity darkening on the back portions of the contact Roche lobes. Larger observational scatter is apparent around Min I, due to high air masses and the faintness of the variable at the time ($\sim 12^{m}.8$).

The O'Connell Effect (O'Connell 1951) is significant at the 3 or 4σ level, $0^{m}.05$, $0^{m}.06$, $0^{m}.05$, and $0^{m}.04$ in B, V, R, and I, respectively, in the sense of Max II–Max I. This logically may indicate either a large cool spot facing the observer near phase $0^{p}.75$ or a hot spot (e.g., a facula) near $0^{p}.25$. The asymmetry is rather broad, affecting the light curve over a range of $\sim 0^{p}.18$. Although conventional wisdom would cause us to choose the cool spot alternative, since dynamo driven magnetic fields arising from rapidly rotating convective components would likely induce them, we decided to explore both possibilities.

One clue to this puzzle is found by comparing the eclipse depths and the general shape of the 1987 curves of Samec & Bookmyer (1987a). (These data are available upon request from the lead author of this article.) The relative shape of these partial curves match our present curves in Min II and in the shoulder leading to Max II (there is a gap in the data from $\sim 0^{p}.63$ to $\sim 0^{p}.09$). The primary maximum, which is well covered, is lower than our present observations, but matches our Max II. This seems to indicate that, had the earlier curves been complete, they would have been *symmetrical* and may represent *immaculate* or unspotted light curves. Thus, out of the four maxima noted, only our Max I is unique, and it exhibits a greatly enhanced light level thus giving evidence for a hot spot. The actual delta magnitudes no longer match, but are consistently larger in the present curves (fainter) by about $0^{m}.075$, $0^{m}.077$, $0^{m}.062$, and $0^{m}.070$ in ΔB, ΔV, ΔR, and ΔI, respectively. This may indicate that the variable is appreciably fainter (by some 7% in V), that the comparison star is brighter or the presence of obscuring circumbinary material. The dimming of the variable by this amount would support the presence of heavy dark spot activity. From the delta magnitudes given above, however,

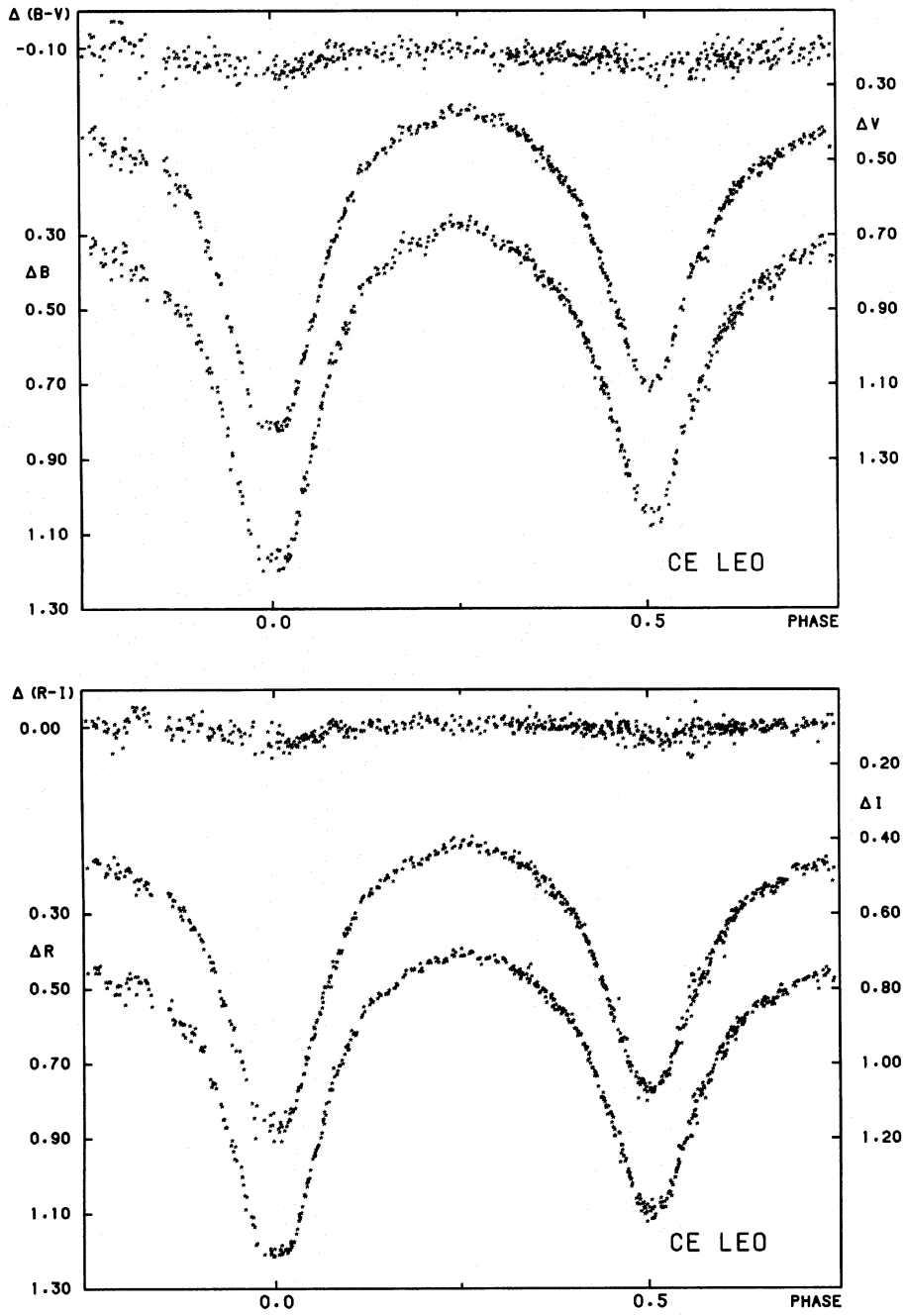

FIG. 4. *B*, *V*, *R*, and *I* light curves of CE Leo as defined by the individual observations listed in Table 1.

we see that the temperature sensitive $\Delta(B-V)$ and $\Delta(R-I)$ values are slightly decreased (indicating higher temperatures) but not at a statistically significant level, so we can learn little from these differential magnitudes about the nature of the temperature difference producing the O'Connell effect. The rapid development of this area (in just 2 yr) is similar to that for active areas which produce dark, i.e., cool regions on the photospheres of stars known to have strong dynamo action (Olah *et al.* 1991).

Specific characteristics of the ΔB, ΔV, ΔR, and ΔI light curves appear in Table 4. Magnitudes displayed in this table represent either averages over small intervals (typically $0^{P}02$) or those determined from a freehand curve carefully fitted to the observations.

6. PHOTOMETRIC SOLUTIONS

Preliminary synthetic light curve solutions were done with the last released, 1983, version of the Wilson–Devinney (W–D) Code, first presented by Wilson & Devinney (1971). Our final solutions and the star spot parameters were computed using the new, yet unreleased

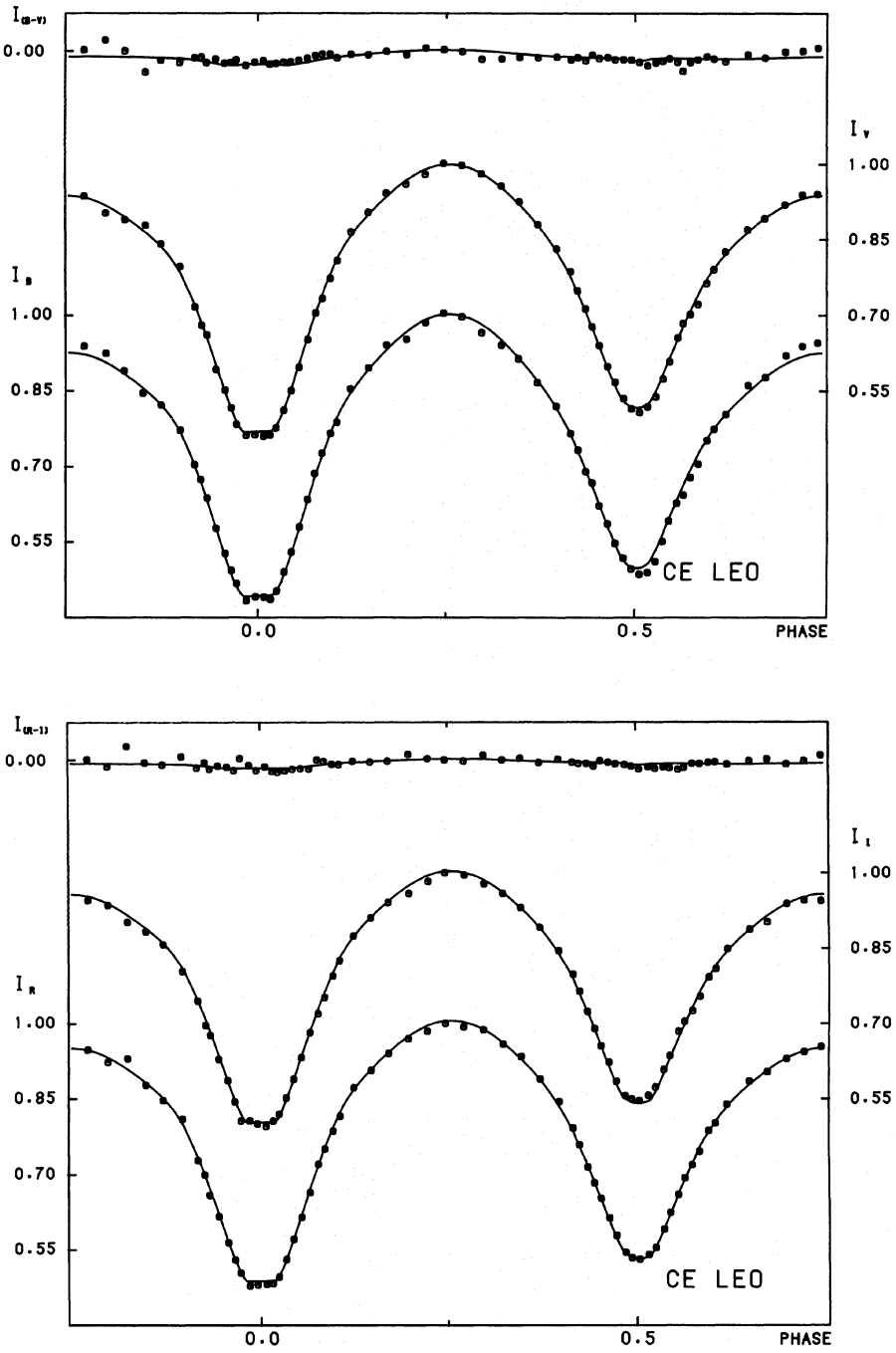

FIG. 5. *B*, *V*, *R*, *I* intensity light curves as defined by observations (normal points) and computed light curves (Model I, with cool spot) for CE Leo.

(as of 1992 May), Wilson–Devinney (Wilson 1990) synthetic light curve code which has the capability of automatically adjusting star spots. In order to reduce the computational time on the Butler University VAX 6610, and to smooth out the scatter in the maxima, normal points were generated. Sixty-four were calculated in units of intensity at each effective wavelength with bin widths of $0^{p}025$ in the out-of-eclipse portions of the light curve and $0^{p}01$ in the eclipse portions. Each normal was weighted according to the number of observations within it. The *B*, *V*, *R*, *I* light curves were solved simultaneously in order to better fix temperature-related phenomena such as light values and surface temperatures. Each curve was then weighted in accordance with the standard deviation of a single observation in the light curves. In the W–D code, synthetic light curves are computed with LC program while the differential corrections procedure is done using the DC program. Blackbody radiation laws were used for both components.

TABLE 4. Light-curve characteristics of CE Leonis.

Delta Mag at Minima and Maxima

Phase	0.00 (MinI)	0.25 (MaxI)	0.50 (MinII)	0.75 (MaxII)
ΔB	1.1728	0.273	1.058	0.327
ΔV	1.211	0.370	1.107	0.433
ΔR	1.206	0.406	1.095	0.454
ΔI	1.174	0.412	1.070	0.457
Δ(B-V)	-0.038	-0.098	-0.049	-0.106
Δ(R-I)	0.031	-0.007	0.025	-0.003

Comparison of Minima

	I	II	Diff.
Depth (B) from Max. at Phase 0.25:	0.900	0.785	0.115
Depth (B) from Max. at Phase 0.75:	0.845	0.730	0.115
Average Depth (B):	0.873	0.758	0.098
Depth (V) from Max. at Phase 0.25:	0.840	0.736	0.104
Depth (V) from Max. at Phase 0.75:	0.778	0.674	0.104
Average Depth (V):	0.809	0.705	0.104
Depth (R) from Max. at Phase 0.25:	0.800	0.690	0.110
Depth (R) from Max. at Phase 0.75:	0.751	0.641	0.110
Average Depth (R):	0.776	0.666	0.110
Depth (I) from Max. at Phase 0.25:	0.762	0.658	0.104
Depth (I) from Max. at Phase 0.75:	0.717	0.613	0.104
Average Depth (I):	0.739	0.636	0.104

Comparison Between Maxima

	B	V	R	I
Difference(0.75 - 0.25) (Max II - Max I)	0.055	0.063	0.485	0.045
Average of Maxima:	0.300	0.402	0.430	0.435

TABLE 5. Synthetic light-curve parameters for CE Leonis.

Parameter	Model I (Cool Spot)	Model II (Hot Spot)
λ_B (nm)	440	440
λ_V (nm)	550	550
λ_R (nm)	640	640
λ_I (nm)	790	790
$x_{1B} = x_{2B}$	0.868	0.868
$x_{1V} = x_{2V}$	0.710	0.710
$x_{1R} = x_{2R}$	0.614	0.614
$x_{1I} = x_{2I}$	0.506	0.506
$g_1 = g_2$	0.32	0.32
$A_1 = A_2$	0.50	0.50
i	87°.60(26)	84°.61(13)
T_1, T_2 (K)	4850 5135(3)	4850, 5111(4)
$\Omega_1 = \Omega_2$	2.841(3)	2.876(4)
q	0.506(2)	0.505(2)
$L_1/(L1+L2)_B$	0.599(1)	0.606(2)
$L_1/(L1+L2)_V$	0.588(2)	0.596(2)
$L_1/(L1+L2)_R$	0.578(2)	0.587(2)
$L_1/(L1+L2)_I$	0.560(2)	0.570(2)
ϕ	0.5009(7)	0.5009(7)
l_3	0.00	0.00
r_1, r_2 (pole)	0.4211(4), 0.3088(12)	0.4149(4), 0.3020(14)
r_1, r_2 (side)	0.4488(5), 0.3235(15)	0.4409(5), 0.3154(17)
r_1, r_2 (back)	0.4801(6), 0.3614(26)	0.4695(5), 0.3488(28)
ρ_1, ρ_2 (g/cm^3)	1.474, 1.858	1.564, 2.028
fillout	15.3%	2.8%
Σwr^2	0.0001882	0.0001638

The noise level integer of the W–D code was set at 2, i.e., the relative weighting of the observations was inversely proportional to the square of the light level (scintillation noise or sky transparency fluctuations). We chose the initial temperature of the primary component, $T_1=4850$ K, consistent with the spectral type determined from the photometry as given in Sec. 3. Linear limb-darkening coefficients, x, were determined from tables by Al-Naimy (1978) and fixed. Standard values of bolometric albedoes, $A=0.5$, and gravity darkening coefficients, $g=0.32$, for convective envelopes were taken from Lucy (1967) and fixed. Mode 3 of the DC program was used in order to make a better determination of the degree of thermal contact.

No previous solutions exist for this system, so we first compared our V light curve to those of our previously solved contact systems and to those given in the Contact Binary Light Curve Atlas of Anderson & Shu (1979). From these initial hints and by trial and error, we found that the set of parameters needed to simulate the observed curves must include a mass ratio of $q \gtrsim 0.5$. Our set of starting parameters used in successfully initiating the DC procedure included $q=0.6$, inclination, $i=88°$, $T_2 \sim 5200$ K, $L_{1B}=8.25$, $L_{1V} \sim 8.5$, $L_{1R} \sim 8.45$, $L_{1I} \sim 8.3$, and surface potential $\Omega=3.0$. Since the DC procedure converges faster when q is less than 1, we introduced a phase shift, $\phi=0^p.5$. The value, ϕ, was adjusted the first few runs to allow for phasing errors within the light curves.

We started by assuming that the system had a dark spot on the cooler component, so we sought parameters which matched the curve everywhere, except at Max II. Consequently, before beginning the procedure, we removed the normal points in the area of the assumed (dark spot) asymmetry, from $\sim 0^p.55$ to $\sim 0^p.87$. A solution was obtained by simultaneously adjusting i, T_2, Ω, q, and L_1. Next, the centroid of the spot was calculated and the width of the spot area was estimated from the O–C residuals of the solution. The spot temperature factor ($T_{\rm spot}/T_{\rm photosphere}$) was varied along with additional changes in spot width until we attained what appeared to be a good fit to the observations. Next, we reinserted the formerly removed normal points and attempted to readjust the star parameters with the addition of the spot, but perhaps due to peculiarities in our particular VAX system, the program kept blowing up. Since we could not identify the problem, the calculations were resumed at the University of Florida by D.T. using the new version of the Wilson–Devinney code. This code has the option of having spot parameters adjust in the DC procedure. The parameters adjusted without mishap. DC converged to the dark spot solution given as Model I in Table 5. The corresponding spot parameters are given in Table 6. The W–D code assumes circular spots of homogeneous surface brightness specified by four parameters—latitude, longitude, radius, and temperature. In this table, spot longitude is the angle measured clockwise as seen from the North Pole from the meridian along the line of star centers. The angle is measured from the direction of the observer at primary eclipse (with our $\phi=0.5$ convention). The computed light curves are shown

TABLE 6. Starspot parameters for CE Leo.

Spot	Cool Spot Model I	Hot Spot Model II
Location	Primary	Primary
Colatitude	90° (fixed)	90° (fixed)
Longitude	94°.52(1)	263°.5(4)
Spot Radius	33°(4)	45°(4)
Temperature Factor	0.93(2)	1.035(4)
Spot Temperature (K)	4525(77)	5019(15)
Spot Area (%)	10	18

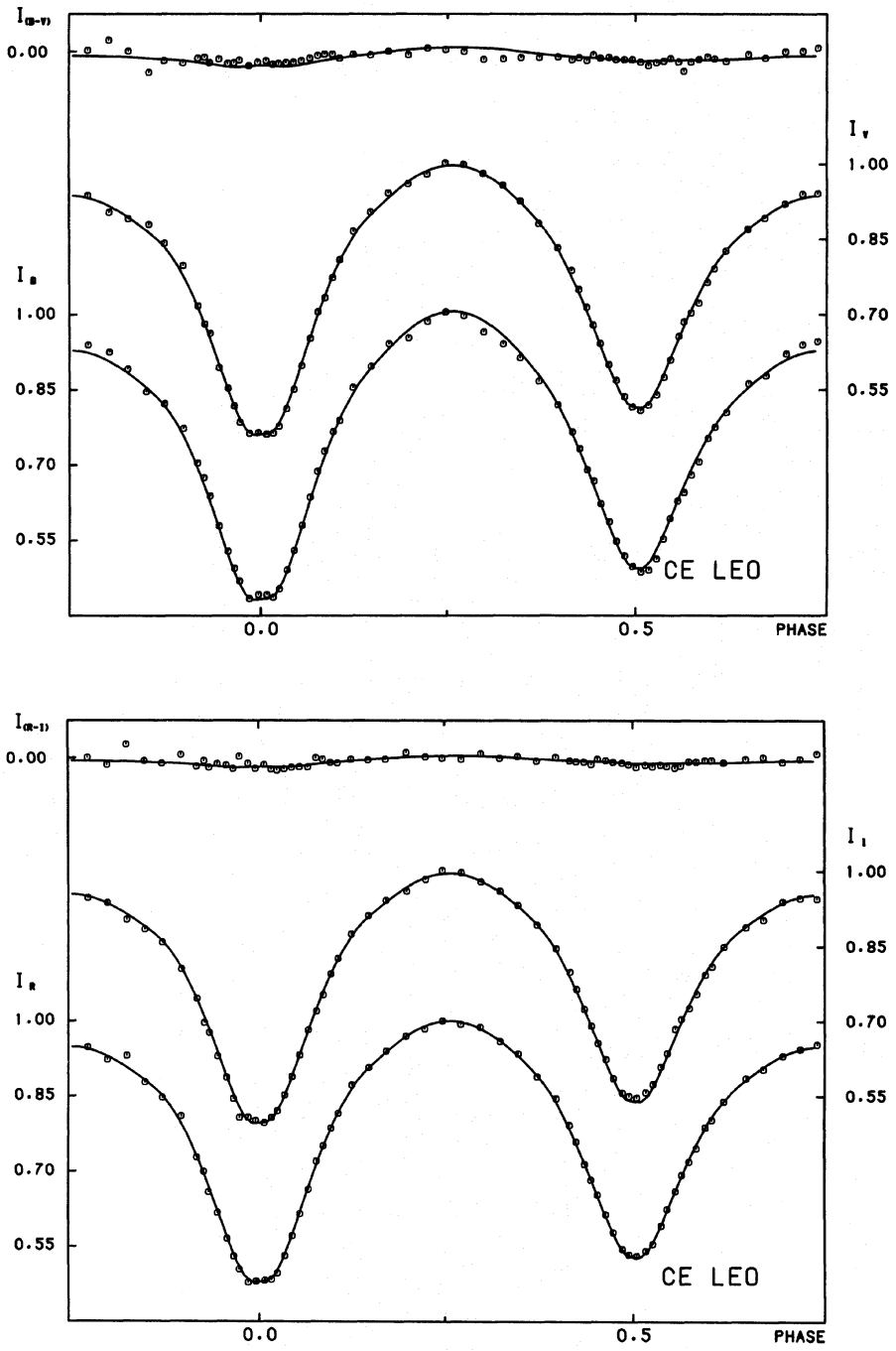

FIG. 6. *B, V, R, I* intensity light curves as defined by observations (normal points) and computed light curves (Model II, with hot spot) for CE Leo.

as Fig. 5. The synthetic light curves do not match our observations in the eclipse portions well.

Next, we tested the suitability of a hot spot solution by displacing the spot by 180° in longitude and then allowing the parameters to readjust. The DC program immediately adjusted the spot temperature factor to >1 and the spot radius to $>40°$. Star parameters were adjusted also. However, due to the high correlations present, especially between spot size and spot temperature, the parameters were divided into the multiple subsets {spot size}, {longitude}, {temperature factor}, $\{i,T_2\}$, and $\{\Omega,q\}$. Each subset was allowed to adjust separately. The same procedure was followed in the calculation of Model I. The solution was very well-behaved and took about twenty iterations to converge. It is given in Table 5 as Model II and the corresponding hot spot parameters included in Table 6. The computed light curves are shown as Fig. 6 and the geometric representation of CE Leo at $0^{p}25$ with the spot

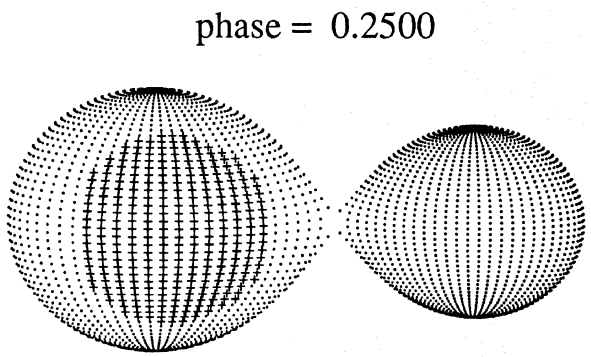

FIG. 7. Geometrical representation of CE Leo at $0^{p}.25$.

is shown in Fig. 7, where the Roche lobe surface was produced by the MAC version of Binary Maker (Bradstreet 1990). Densities and fill-outs in Table 6 were also calculated using Binary Maker. The Σwr^2 residual for the hot spot solution is about 13% lower than that for the dark spot solution, attesting to the better overall fit of this model (especially in the eclipses). The ability to adjust spots by the differential corrections procedure must be an improvement over hand-modeled ones. We suggest that light curves with large O'Connell effects should have their spot parameters rechecked with the new W–D code.

7. DISCUSSION

The photometry, in conjunction with our lowest residual, Model II, solution for CE Leo indicates that the system consists of two early spectral K-type stars (K1 and K2) with a mass ratio of $\sim$0.5 in a state of marginal contact and a temperature difference, $\Delta T = 260$ K. However, we must remember when discussing determinations of spectral types of rapidly rotating stars, that the $B-V$ color index may be reddened by up to $0^{m}.20$ and that the V magnitude may be reduced correspondingly, by $1^{m}.05$ in equatorial zones of single solar type stars (Faulkner *et al.* 1968). The fill-out factor of 3% was somewhat low for W UMa W-type binaries, which usually fall in the 10% to 20% range. Since Guinan & Bradstreet (1988), in their kinematical–statistical study of W UMa systems, detect a weak positive correlation between space velocity (i.e., kinematical age) and fill-out, this indicates that CE Leo may have recently come into contact. However, CE Leo must have been in physical contact long enough to develop good thermal contact as indicated by the small ΔT, i.e., its EW light curve. Most theories of the evolution of contact binaries predict that q decreases with increasing contact age. Mass ratios for F or earlier spectral type W UMa-type systems generally fall in the 0.2 to 0.6 range, and the q value for CE Leo falls in the upper one-third of modeled systems (e.g., see lists in Guinan & Bradstreet 1988, Mochnacki 1985, 1981, and Van Hamme 1982). The above average mass ratio determined for CE Leo is in support of the notion that it has recently come into contact due to the angular momentum loss of this spot-active binary. (The photometric q value is well determined in this case, since the light curves display complete eclipses and both models yield, statistically, the same value.) Also we found a possible constant period decrease which, if verified, would mean there has been a decreasing separation of the components.

TABLE 7. Comparison of hot spot regions.

System	Max. Phase	~Size	T Factor	Type	Fill-out	Source
EH Hya	$0^{p}.35$	$0^{p}.10$	1.25	SC	12%	RC
V865 Cyg	$0^{p}.35$	$0^{p}.15$	1.32	SC	17.5%	SH
SS Ari	$0^{p}.36$	$0^{p}.10$	1.10	SC	13%	WL
VW Boo	$0^{p}.38$	$0^{p}.20$	1.11	SC	19%	PR
CE Leo	$0^{p}.23$	$0^{p}.20$	1.04	SC	3%	PO
RR Lep	$0^{p}.18$	$0^{p}.10$	1.04	NC	-16%,0%	SF

Note: SC = Shallow Contact, NC = Near Contact.
RC = Samec et al. 1991, SF = Samec et al. 1989a,
SH = Samec et al. 1992, WL = Lu 1991,
PO = Present Observation, PR = Rainger, et al. 1990

The density of the primary star is near that of a G5 (V) main-sequence star while the density of the secondary component is consistent with its photometrically determined K1 (V) spectral type. However, both rapid rotation and the energy enhancement of the secondary by the primary could "mask" the true identity (the mass) of the components. In W-type systems, the secondary is overluminous and the primary component is underluminous for their mass. Evidently, an energy exchange takes place with the secondary component gaining energy at the expense of the primary component. If we assume that the primary and secondary components are similar to $\sim$G5 (V) and $\sim$M0 (V) single main-sequence stars, from the present energy enhancement of the secondary (including a small correction for rotational reddening) we calculate reasonably well, using simple blackbody physics, the present temperature of the primary. Therefore, we suspect that just prior to contact, the system consisted of stars close to these spectral types.

Of interest is the possible presence of a large hot spot region on the cooler component of the binary. In Table 7, we list six other short period eclipsing binaries whose light curves have recently been solved using hot spots. For near contact, semidetached systems, like RR Lep (Samec *et al.* 1989), the occurrence of a hot spot is easily explained by a gas stream leaving the L1 point of the secondary component, striking the surface of the primary component (Richards 1992). Superluminous areas on contact systems may be explained as the result of matter in transit through the "neck" of the Roche lobes accelerating toward the other component causing an acoustic shock wave, thus heating up the photosphere (Lu 1991). Of course, we cannot discount the idea that light variations are magnetic in nature. Indeed, Guinan (1990) has suggested that chromospherically active stars could be dominated by white light faculae more than by dark spots. Although Guinan refers to the overall light variation of systems, we feel that extensive remodeling of contact systems with hot spots may, in fact, indicate that this type of activity may be

wide-spread or even more prevalent than dark spot activity. In passing, we note, without explanation, that there is a rough correlation between the fillouts of systems listed in Table 7 and the positions of the hot spots, with the higher fillouts having a shift in phase toward 0^P5.

Whatever the cause, whether fluid hydrodynamics or magnetic spot activity or a combination of both, or whatever the rate of occurrence of hot spots, we believe that the photometry presented here at least *suggests* the presence of a very large superluminous area on CE Leo and that researchers in the field should be cognizant of this interpretation. Doppler imaging (Maceroni *et al.* 1991; Noah 1987) of contact binaries should help resolve this hot versus cool spot question.

We would like to thank Dr. Kwan-Yu-Chen of the Department of Astronomy, University of Florida for the continued maintenance of the *University of Florida Card Catalog of Interacting Binaries* which we have used extensively for its bibliographical information and lists of timings of minimum light. In addition, we are especially grateful to the library staff of the U.S. Naval Observatory and particularly, to Mrs. Brenda G. Corbin, head librarian, for tracking down many and possibly obscure but important references for this and previous research articles. We wish to thank Butler University for the awarding of an internal grant to W.S., making it possible for her to study CE Leo and to present the results of her work at the 1992 Indiana Undergraduate Research Conference. Also, we wish to thank Dr. Peter B. Boyce and the American Astronomical Society Small Research Grant Committee and NASA for their partial support of this research. The research of R.G.S. and W.S. was supported partially by a 1988–1989 Faculty Butler University Academic Fellowship Grant and a 1991–92 Summer Student Research Grant. R.G.S. was also supported partially by a grant from NASA administered by the American Astronomical Society.

REFERENCES

Al-Naimy, H. M. 1978, Ap&SS, 53, 181
Anderson, L., & Shu, F. H. 1979, ApJS, 40, 667
Bessell, M. S. 1976, PASP, 88, 557
Bessell, M. S. 1979, PASP, 91, 589
Bradstreet, D. H. 1990, BAAS, 22, 1293
Derman, E., & Demircan, O. 1992, AJ, 103, 1658
Eggen, O. J. 1967, MNRAS, 70, 111
Faulkner, J., Roxburgh, I. W., & Strittmater, P. A. 1968, ApJ, 151, 203
Guinan, E. F. 1990, in Proceedings of the International Symposium on Evolution in Astrophysics, ESA SP-310, p. 73
Guinan, E. F., & Bradstreet, D. H. 1988, in NATO Advanced Study Institute on the Formation & Evolution of Low Mass Stars (Kluwer, Dordrecht), p. 345
Hall, D. S. 1990, in Active Close Binaries, edited by C. Ibanoglu (Kluwer, Dordrecht), p. 95
Hall, D. S. 1991, ApJ 380, L85
Hardie, R. H. 1962, Stars & Stellar Systems, Vol. 2, Astronomical Techniques (University of Chicago Press, Chicago), p. 18
Hertzsprung, E. 1928, Bull. Ast. Int. Neth., 4, 179
Hoffmann, M. 1983, IBVS No. 2344
Hoffmann, M. 1984, V. Bonn. 96, 1
Hoffmeister, C. 1963, AN, 287, 169
Hut, P., *et al.* 1992, PASP, 681, 981
Kreiner, J. M. 1977, IAU Colloquium No. 42, 373
Landolt, A. U. 1983, AJ, 88, 439
Lipari, S. L., & Sistero, R. F. 1987, AJ, 94, 792
Lloyd, C., Watson, J., & Pickard, R. D. 1992, IBVS No. 3704
Lu, W. 1991, AJ, 102, 262
Lucy, L. B. 1967, Zs. f. Ap., 65, 89
Maceroni, F., Van 'T Veer, F., & Vilhu, O. 1991, The Messenger, 66, 47
Meinunger, L., & Wenzel, W. 1968, VSS 7 (4), 430
Mochnacki, S. W. 1983, in Interacting Binaries (Reidel, Dordrecht), p. 51
Mochnacki, S. W. 1985, ApJ, 245, 650
Noah, P. V. 1987, dissertation, The University of Toledo
Olah, K., Hall, D. S., & Henry, G. W. 1991, A&A, 251, 531
O'Connell, D. J. K. 1951, Pub. Riverview Coll. Obs. 2, 85
Popper, D. M. 1980, ARA&A, 18, 115
Rainger, P. P., Bell, S. A., & Hilditch, R. W. 1990, MNRAS, 246, 47
Richards, M. T. 1992, BAAS, 24, 770
Samec, R. G. 1990, AJ, 100, 808
Samec, R. G., & Bookmyer, B. B. 1987a, IBVS No. 3053
Samec, R. G., & Bookmyer, B. B. 1987b, PASP, 99, 1298
Samec, R. G., Charlesworth, S. D., & Dewitt, J. R. 1991, AJ, 102, 688
Samec, R. G., Fuller, R. E., Bookmyer, B. B., & Faulkner, D. R. 1989, PASP, 101, 180
Samec, R. G., & Hube, D. P. 1991, AJ, 102, 1991
Tout, C. A., & Hall, D. S. 1991, MNRAS, 253, 9
Van Hamme, W. 1982, A&A, 105, 389
Wenzel, W., & Zeigler, E. 1966, MVS 4(2), 20
Wilson, R. E. 1990, ApJ, 356, 613
Wilson, R. E., & Devinney, E. J. 1971, ApJ, 166, 605